AD A111121

LEVEL Ⅱ ①

FEB 19 1982

DEPARTMENT OF THE AIR FORCE
AIR UNIVERSITY (ATC)
# AIR FORCE INSTITUTE OF TECHNOLOGY

Wright-Patterson Air Force Base, Ohio

82 02 18 137

NONLINEAR PARAMETER IDENIFICATION:
LIFT COEFFICIENT, DRAG COEFFICIENT,
AND BANK ANGLE HISTORIES FOR THE
SPACE SHUTTLE TEST FLIGHT I

THESIS

AFIT/GA/AA/81D-7     Harry F. Johnson
                     2d Lt        USAF

NONLINEAR PARAMETER IDENTIFICATION:

LIFT COEFFICIENT, DRAG COEFFICIENT, AND

BANK ANGLE HISTORIES FOR THE SPACE SHUTTLE

TEST FLIGHT I

THESIS

Presented to the Faculty of the School of Engineering

of the Air Force Institute of Technology

Air University

in Partial Fulfillment of the

Requirements for the Degree of

Masters of Science

by

Harry F. Johnson, B.S.

2d Lt          USAF

Graduate Astronautical Engineering

December 1981

## Preface

The computer program that I used to get my results may be helpful to anyone interested in programming a similar optimization technique. A copy is available through the Astronautical Engineering Department of the Air Force Institute of Technology.

# Contents

# List of Figures

# List of Tables

## List of Symbols

<u>Roman Letter Symbols</u>

| | | |
|---|---|---|
| $A$ | – | Algorithm convergence variable |
| $B$ | – | Algorithm convergence variable |
| $C_D$ | – | Drag coefficient |
| $C_L$ | – | Lift coefficient |
| $g$ | – | Gravity (ft/sec$^2$) |
| $G_K$ | – | Computed state vector at time k |
| $H$ | – | Algorithm matrix $SS^T$ |
| $h_{RW}$ | – | Runway altitude above sea level (ft) |
| $J$ | – | Performance index |
| $J_\beta$ | – | Derivative of J with respect to $\beta$ |
| $\lambda$ | – | Number of time increments |
| $L$ | – | Lift (lb) |
| $L_Z$ | – | Lift in the z direction (lb) |
| $m$ | – | Mass (slug) |
| $R_\epsilon$ | – | Radius of the Earth |
| $s$ | – | Reference area (ft$^2$) |
| $S$ | – | Algorithm update matrix |
| $t$ | – | Time (sec) |
| $v_Z$ | – | Velocity in the z direction (ft/sec) |
| $V$ | – | Velocity vector (ft/sec) |
| $w$ | – | Weight (lb) |
| $W$ | – | Algorithm weighting matrix |

## List of Symbols

### Roman Letter Symbols

$x_1$ — State vector element in the x coordinate distance (ft)

$x_2$ — State vector element in the y coordinate distance (ft)

$x_3$ — State vector element in the z coordinate distance (ft)

$x_4$ — State vector element for velocity magnitude (ft/sec)

$x_5$ — State vector element for azimuth

$x_6$ — State vector element for flight path angle (rad)

$x_{1d}$ — Radar or BET x coordinate distance (ft)

$x_{2d}$ — Radar or BET y coordinate distance (ft)

$x_{3d}$ — Radar or BET z coordinate distance (ft)

$x_{4d}$ — Radar or BET velocity (ft/sec)

$x_{5d}$ — Radar or BET azimuth angle (rad)

$x_{6d}$ — Radar or BET flight path angle (rad)

$\bar{X}$ — State vector

$Y_k$ — Experimental state vector at time k

### Greek Letter Symbols

$\alpha$ — Algorithm one-dimensional search variable

$\beta$ — Vector with parameter history polynomial coefficients as elements

$\epsilon$ — Numerical differentiation constant

$\gamma$ — Flight path angle (rad)

$\mu$ — Bank angle (rad)

$\nu$ — Algorithm variable

$\chi$ — Azimuth angle (rad)

## Abstract

A nonlinear, Square-Root Variable-Metric optimization technique is used to extract time histories for the lift coefficient, drag coefficient, and bank angle control variables from radar data of the Space Shuttle Test Flight. I. This optimization technique solves for these control variable histories by minimizing a weighted least squares performance index of the calculated versus experimental state equation time histories. The state model is a three degree of freedom representation of aircraft motion.

Three intervals of data are evaluated. In each interval, polynomial functions represent the control variables, and the peformance index is dependent only on the values of the polynomial coefficients. The larger of the first two intervals contained the shorter interval so that the effect of changing polynomial order and interval length could be explored. The third interval compared the calculated parameter histories with NASA's BET parameter histories with good correspondence. For all three intervals the calculated state histories closely matched the experimental state histories.

These results show that given an appropriate state model, this optimization technique is useful for quickly obtaining good and inexpensive estimates of certain desired parameters.

NONLINEAR PARAMETER IDENTIFICATION:

LIFT COEFFICIENT, DRAG COEFFICIENT, AND

BANK ANGLE HISTORIES FOR THE SPACE SHUTTLE

TEST FLIGHT I

## I Introduction

Evaluating the performance of a new and technologic-
ally advanced engineering system requires a thorough, and
often redundant, study of test data. Agreement between
these different studies helps to reinforce any conclusions
derived from the tests. The Space Shuttle Test Flights
will, accordingly, be very well studied and documented.
The Space Shuttle trajectory is computed several different
ways, and this data enables important parameters, such as
lift coefficient, drag coefficient, and bank angle histories,
to be determined. These parameter histories give insight
into the performance of the Shuttle, so that expected
performance parameters can be evaluated for their accuracy.

NASA computes a "Best Estimated Trajectory" (BET)
(Ref 7), containing estimates of the parameter histories,
by using the data from the Aerodynamic Coefficient
Instrumentation Package (ACIP), which is on board the Space
Shuttle, and various radar data. The ACIP gives gyro and
accelerometer data, whereas the radar gives optical and
telemetry data. This data is combined, through a linear

stochastic estimation process, to produce an optimal six degree of freedom (DOF) model of the *Space Shuttle's* trajectory (Ref 3, 4, 5, 6).

Although NASA's BET is a good method for estimating the trajectory and motion of the Space Shuttle, it may take a few months to synthesize all of the available data into a BET. Yet the radar data, such as the data from the Multisensor Space Position Report (Ref 8:1), is sufficient to calculate three DOF trajectories and performance parameters, such as $C_L$, $C_D$, and $\mu$. This report proposes a simple and inexpensive computer algorithm to evaluate this data and come up with a good estimate of some of the performance parameters of the Space Shuttle. This could provide an on-line estimate, which evaluates the radar data as it comes in. Its results could be compared to the BET in post data analysis, which would help locate possible software errors in the two estimation procedures and be used to confirm wind tunnel data. The immediate results would also be useful in evaluating the trajectory should anything go wrong during the final landing phase of reentry.

## Problem Statement and Method

This report tests a parameter estimation method which can be used to evaluate the Space Shuttle radar data as it becomes available. The method proposed is a slightly modified Davidon-Fletcher-Powell (DFP) optimization technique

2

derived by Williamson and Hull (Ref 4:1).  The dynamical system from which the parameters are identified can be closely approximated without the need for linear stochastic noise modeling by using a deterministic nonlinear state model (Ref 4).  The DFP variable-metric method, using such a model, is an efficient, quasi second-order numerical algorithm that minimizes a performance index.  This performance index is calculated from a weighted least squares fit of the calculated onto the experimental (radar data) state histories.  The calculated state histories are dependant upon the parameter histories through the coefficients of a polynomial fitted to each parameter history.  These coefficients are the variables that are changed to minimize the performance index.  The parameter histories that this report identifies are the lift coefficient, the drag coefficient, and the bank angle histories.

The data used to calculate the performance index came from two sources.  The first set of data came from the Mulitsensor Space Position Report (Ref 8:1).  Its trajectory histories supply sufficient information to derive the time histories of the parameters $C_L$, $C_D$, and $\mu$ through some optimization technique, such as the algorithm in this report. As this algorithm was being evaluated using the Multisensor Report data, the NASA BET data became available.  Although the BET data was itself derived from a parameter estimation process, it contains trajectory history data as in the

Multisensor Report.  The parameter histories obtained by
the algorithm using these trajectory histories were compared
to the BET parameter histories.  The degree of correspondence
between these parameter histories provides a measure of the
accuracy of the algorithm.

## Organization

Chapter II discusses the procedure used to extract the
parameters from the radar data.  This will include a descrip-
tion of the Square-Root Variable-Metric algorithm and an
explanation of the mating of the state equations and data.
Chapter III explains the problems and pitfalls of manipulating
the algorithm to provide the best results.  Chapter IV presents
the results and interprets their significance.  Chapter V
summarizes the report and gives an explanation of the useful-
ness of this parameter identification method.

## II Procedure

### Methods of Parameter Identification

Many techniques have evolved that solve for variables
of interest from some collection of input. Each method has
proven useful at some time, although the degree of accuracy
between methods varies greatly. For instance, the BET gives
accurate parameter estimations given all of the available
data. Yet it was a time-consuming process to get the BET.
On the other hand, there are gradient optimization techniques
that are quick and inexpensive, yet only crudely approximate
the parameters. But there are certain common characteristics
of parameter estimation methods for a dynamical system. Hull
and Williamson (Ref 4:1) explain:

> In general, the parameter estimation problem
> for a dynamical system consists of finding the
> values of a set of p constants C and n initial
> states $X_0$ (assuming $t_0=0$) such that the solution
> of the dynamical system

$$\dot{X} = F(t, X, C) \tag{1}$$

fits the experimental data. The data is fit by

5

minimizing the weighted least squares performance
index

$$J = \sum_{K=1}^{\ell} \left( Y_K - G_K \right)^T W \left( Y_K - G_K \right) \qquad (2)$$

were the subscript k denotes the time at which
the experimental data is taken and W is a positive-
definite diagonal matrix whose elements are the
inverses of the measurement convariance. The
quantity Y is a q-vector of the experimental values,
and G is q-vector of computed values which is related
to the state of the dynamical system, that is,
$G = G(t,X)$.

The technique of parameter identification proposed in
this report is a compromise between the crude and the sophis-
ticated methods. It is a nonlinear method, which implies
that the state equations would exactly map the motion if the
three DOF model was an exact representation of the real
world. The Square Root Variable-Metric algorithm of
Williamson's (Ref 9:107) chooses $\beta = [X_O \ C]^T$, where $X_O$ is
the initial state vector and C is a vector of constants
associated with the parameter histories, to minimize the

6

weighted least squares performance index. The algorithm is:

1. Guess $\beta$ and a positive-definite, symmetric matrix S. Compute $J(\beta)$, $J_\beta(\beta)$ (the derivative of the performance index with respect to $\beta$) and $H = SS^T$.

2. Compute the change in $\beta$ from the formula

$$\Delta \beta = - \propto HJ^T \tag{3}$$

using a one-dimensional search to determine the scalar step size $\propto$ which minimizes $J$ in the $-HJ^T$ direction. This search yields a new function value $\bar{J}$, where

$$\bar{J} = J(\beta + \Delta\beta) \tag{4}$$

3. Compute a new gradient $\bar{J}_\beta^T$ and form the difference

$$\Delta J^T = \bar{J}_\beta^T - J_\beta^T \tag{5}$$

4. Compute a new metric $\bar{H}$ from the relation

$$\bar{H} = \bar{S}\bar{S}^T \tag{6}$$

where

$$\bar{S} = S[I - (\mathcal{V}/A)S^TYY^TS] \tag{7}$$

$$A = Y^T H \Delta J_\beta^T, \quad Y = \propto J_\beta^T + \Delta J_\beta^T$$

$$\mathcal{V} = [1+(1-B/A)^{\frac{1}{2}}] / (B/A), \quad B = Y^TSS^TY$$

If $\mathcal{V}$ is imaginary, use $\mathcal{V} = 1$ in the above expression for $\bar{S}$.

5. If the process has not converged, repeat the procedure. Convergence has occurred when $\propto \to 1$, $A \to 0$ and $B \to 0$ simultaneously.

Since the metric H is calculated as the S matrix times its transpose, it will always be positive definite. The positive definiteness of H means the performance index will decrease on every iteration, regardless of the accuracy in calculating the S matrix. Likewise, the one-dimensional

alpha search need not be extremely accurate, as is necessary

with the unmodified DFP algorithm, to maintain a positive

definite H.

## Numerical Integration and Differentiation

The method used to numerically calculate $J(\beta)$ is as

follows:

1. Guess values for $X_O$ and C to give $\beta = [X_o \ C]^T$.

2. Compute $Y_O - G(t_O, X_O)$ from guessed $X_O$. (Note that in this report the initial state vector $X_O$ was assumed to be equal to $Y_O$ and $\beta$ was therefore $\beta = [C]^T$.)

3. Integrate $\dot{X} = F(t, X, C)$ from $t_O$ to $t_1$. This enables $Y_1 - G(t_1, X_1)$ to be computed. In this manner, integrate $X$ and calculate $Y_K - G(t_K, X_K)$ until the final time (the last observation) is reached.

4. Using Eq. (2), compute $J(\beta)$.

The gradient of $J(\beta)$, $J_\beta(\beta)$, is a vector calculated

through numerical differentiation by perturbing each element

of $\beta$ and differencing the performance indexes that are calcu-

lated using the perturbed $\beta$ vectors. The central difference

formula

$$J_{\beta_j} = \left[ J\left(\beta_1, \beta_2, \ldots, \beta_j + \delta\beta_j, \ldots, \beta_{p+n}\right) - J\left(\beta_1, \beta_2, \ldots, \beta_j - \delta\beta_j, \ldots, \beta_{p+n}\right) \right] / \left(2\,\delta\beta_j\right) \quad (8)$$

is the differencing technique used in this report, where $\delta\beta_j$

is the perturbation in the $j^{th}$ element of $\beta$. This means

that each element of $J_\beta$ requires two calculations, and hence

two integration loops, for J. The central difference formula

8

was chosen because it is uncomplicated yet provides a truncation error of order $\delta\beta^2$. Therefore, the smaller the $\delta\beta_j$, the better, but there is also a limit to how small $\delta\beta_j$ can be due to computer round-off error.

Hull and Williamson (Ref 4) say that "in order to have the greatest number of correct significant figures in a derivative, it is necessary to select the $\delta\beta$ which causes the largest change in J while keeping the truncation error of the derivative in check." $J(\beta_j \pm \delta\beta_j)$, and hence $J_{\beta_j}$, are computed using

$$\delta\beta_j = \epsilon |\beta_j| \quad \text{if} \quad |\beta_j| > 1 \tag{9}$$

$$\delta\beta_j = \epsilon \quad\quad\quad \text{if} \quad |\beta_j| \le 1$$

where $\epsilon$ is a prescribed tolerance.

### State Equations

The algorithm uses the following state equations to model the three DOF motion of the Space Shuttle:

$$\dot{x}_1 = x_4 \cos(x_6) \sin(x_5)$$

$$\dot{x}_2 = x_4 \cos(x_6) \cos(x_5)$$

$$\dot{x}_3 = x_4 \sin(x_6)$$

$$\dot{x}_4 = [-w \sin(x_6) - \tfrac{1}{2} C_0 \rho s (x_4)^2] / m$$

$$\dot{x}_5 = \tfrac{1}{2} C_L \rho s x_4 \sin(\mu) / (m \cos(x_6))$$

$$\dot{x}_6 = [\tfrac{1}{2} C_L \rho s (x_4)^2 \cos(\mu) - w \cos(x_6)] / (m x_4)$$

(10-15)
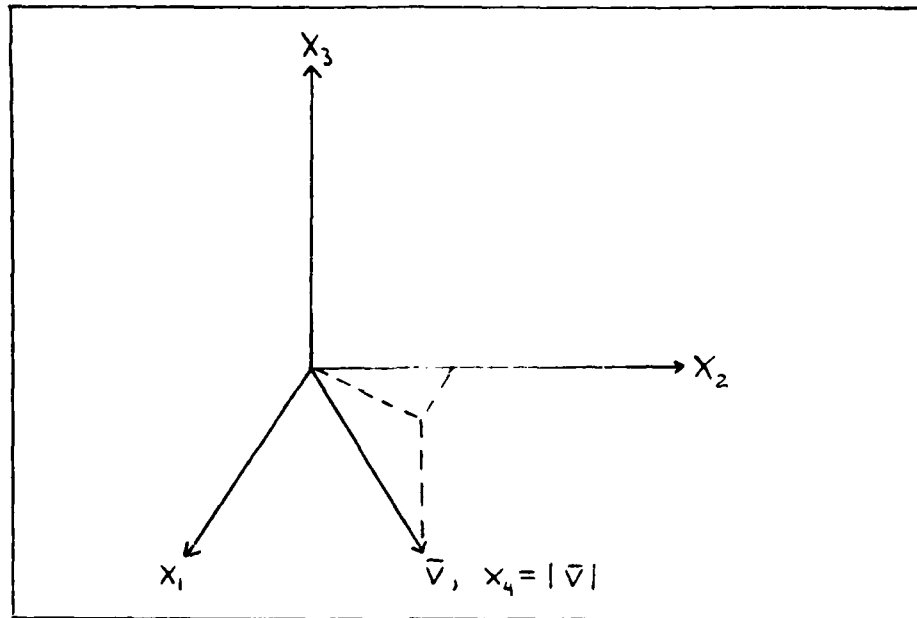
Fig. 1. Flat-Earth Coordinate System

These equations are derived from a flat-Earth coordinate system (Fig. 1) where $x_3$ is the altitude, $x_1$ and $x_2$ are the planar coordinates orthogonal to the altitude such that the coordinate system is right handed. The directions of $x_1$ and $x_2$ depend on which data set is used. The state $x_4$ is the magnitude of the velocity, $x_5$ is the azimuth, and $x_6$ is the flight path angle.

## Data Manipulation

The algorithm requires an experimental trajectory $(Y_K)$ as an input. The $Y_K$ is a time history of the states. The radar data can be manipulated to give state vector values at each time increment k. This report used two sources of radar data to yield $Y_K$, the Multisensor Report data and the

BET data.  The data from the Mulitsensor Report (Ref 8)
was with respect to an Earth Surface Fixed (ESF) Cartesian
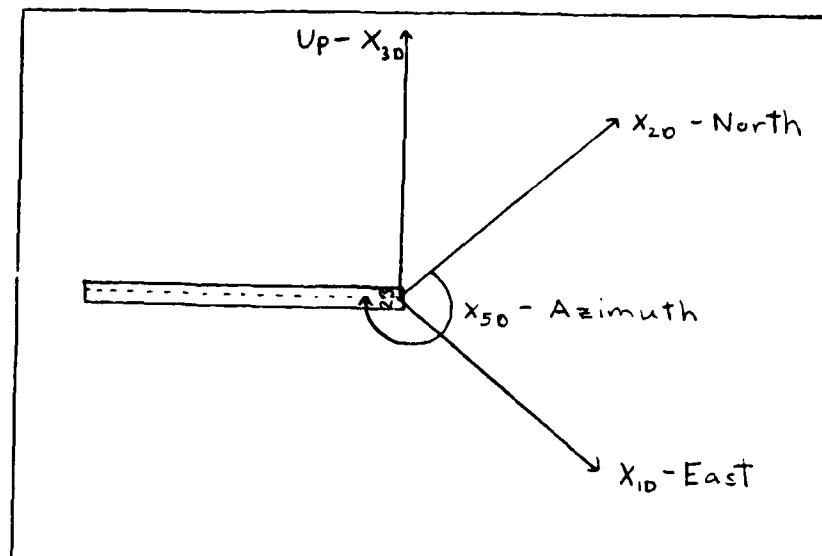


Fig. 2.  Earth Surface Fixed Coordinate System

coordinate system (Fig. 2) which rotates with the Earth.
Because the time intervals evaluated were very short (less
than two minutes in every case), the rotation of the Earth
was ignored in transforming the radar data into $Y_K$.  As
shown in Figure 2, the ESF coordinate system had the
beginning of runway 23, Edwards AFB, as the origin, with the
$x_{1D}$ axis positive East, the $x_{2D}$ axis positive North, and
the $x_{3D}$ axis positive up.  For $Y_K$, the states $x_1$ and $x_2$
were given by $x_{1D}$ and $x_{2D}$ data, respectively.  The azimuth,
$x_{5D}$, was measured from North with the clockwise direction

11

being positive, and the flight path angle, $x_{6D}$, was the angle between the velocity vector and the $(x_{1D}, x_{2D})$ plane. For $Y_K$ the states $x_5$ and $x_6$ were given by $x_{5D}$ and $x_{6D}$, respectively, and $x_4$ was given by the magnitude of the velocity, which the Multisensor Report also provided.

The only state that needed to be calculated from the
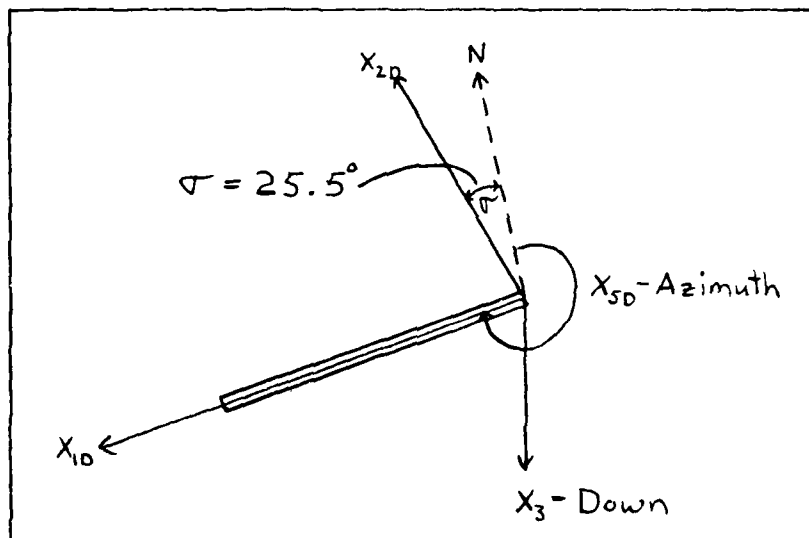


Fig. 3. Runway Coordinate System

given data was $x_3$. The Multisensor Report also provided the altitude of the Space Shuttle. Therefore $x_3$ was given by the Space Shuttle altitude minus the altitude of the runway.

The BET data uses a similar coordinate system (Fig. 3). The $x_{1D}$ axis is positive in the direction of the runway; the

positive $x_{2D}$ axis makes up the third coordinate for the right

handed coordinate system with the $x_{3D}$ axis positive down (Ref 1).

Again, $x_{5D}$, (asimuth) is measured from North, clockwise

positive, and $x_{6D}$ was the angle between the velocity vector

and the ($x_{1D}$, $x_{2D}$) plane. To arrive at state elements $x_1$ and

$x_2$ of $Y_K$ a rotation of 25.5 degrees was added to the $x_5$ term

in each of the $\dot{x}_1$ and $\dot{x}_2$ equations. This gave the $\dot{x}_1$ and

$\dot{x}_2$ equations a corrected azimuth measured from the $x_{2D}$ axis.

Although the Multisensor Report provided the altitude

of the Space Shuttle, for the BET data the altitude, and

therefore $x_3$, the altitude of the Space Shuttle measured

from the origin at runway 23, needed to be calculated using

the cosine formula for triangles

$$x_3 = \left[(R_E + h_{rw})^2 + x_{10}^2 + x_{20}^2 + x_{30}^2 - 2(R_E + h_{rw})(x_{10}^2 + x_{20}^2 + x_{30}^2)^{1/2} \cos\left(-x_{30}/(x_{10}^2 + x_{20}^2 + x_{30}^2)^{1/2} + 90\right)\right]^{1/2} - (R_E + h_{rw}) \quad (16)$$

Figure 4 shows the geometry that this equation was derived

from. This equation is applicable as long as $x_{3D}$ is negative

(Space Shuttle is above the horizon). Since this report is

concerned with data from radar stations along the West Coast,

the problem of $x_{3D}$ positive was not considered. The $x_5$ and

$x_6$ elements of $Y_K$ are given by $x_{5D}$ and $x_{6D}$ respectively.

Finally, the magnitude of the velocity, $x_4$, is calculated

as the square root of the sum of the squares for $\dot{x}_{1D}$, $\dot{x}_{2D}$,

and $\dot{x}_{3D}$ (which are provided by the BET).

13
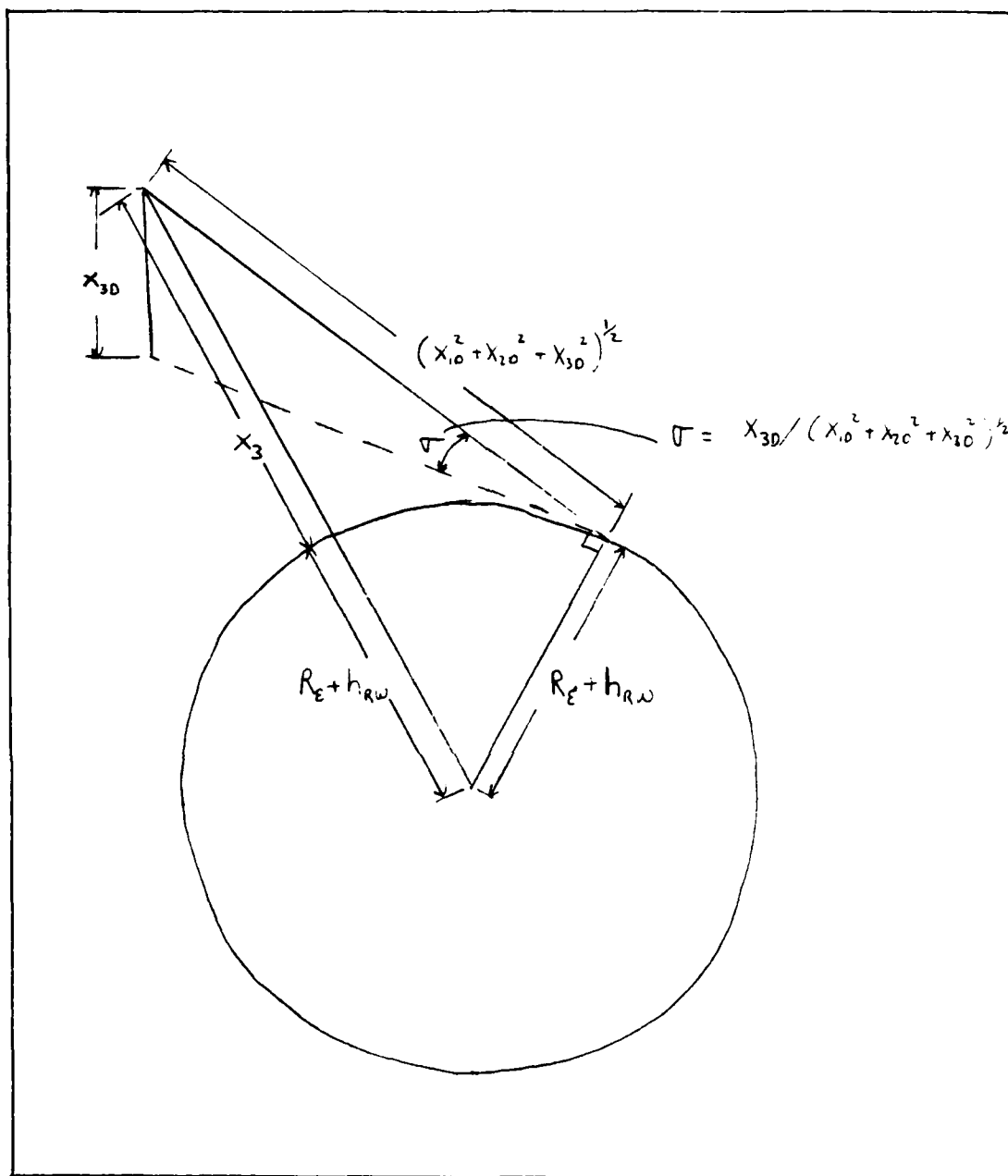
Fig. 4.  Geometry for Calculating $x_3$

## Parameters

The parameter histories of interest are $C_L$, $C_D$, and $\mu$. The algorithm requires initial guesses for these parameter histories. To solve for the initial time history for $C_L$ the equation of motion in the vertical direction

$$L \cos(\gamma) \cos(\mu) - w = m \dot{V}_z \qquad (17)$$

was used. The $\cos(\mu)$ term was chosen to be equal to one. This approximation is based upon the knowledge that $\mu$ for a heavy glider like the Space Shuttle should not exceed 45 degrees, and in most cases it will be below 30 degrees. Therefore, at worst, this is a 70% accurate approximation. Furthermore, $\dot{V}_Z(t_i)$, which is the acceleration in the Z (up) direction at time $t_i$, can be approximated by the central difference formula

$$\dot{V}_z(t_i) = \left( V_z(t_{i+1}) - V_z(t_{i-1}) \right) \Big/ \left( t_{i+1} - t_{i-1} \right) \qquad (18)$$

Therefore, representing L as $\tfrac{1}{2}\rho(t_i) V^2_{z_i} S\, C_L(t_i)$ we have

$$C_L(t_i) = \frac{w\left[ \left( V_z(t_{i+1}) - V_z(t_{i-1}) \right) / (g(t_{i+1} - t_{i-1})) + 2 \right]}{\rho(t_i) S V^2(t_i) \cos(\gamma(t_i))} \quad , \; i = 1, 2, \ldots, n \qquad (19)$$

where n is the length of the time interval of interest divided by the step size taken between data points (n is the total number of data points for each of $C_L$, $C_D$, and $\mu$) and where $\gamma(t_i)$ is the flight path angle at time $t_i$. The air density ($\rho$) history is also derived from a Least Squares polynomial fit to the air density data given by References 7 and 8.

16

For the Multisensor Report data, the $C_D$ time history guess was derived from lift over drag graphs in Reference 1. The $C_D$ history for the BET data was calculated using the lift over drag (L/D) data already available from the BET. However the initial $C_L$ and $C_D$ histories are calculated, the closer they are to the true $C_L$ and $C_D$ the faster the algorithm will converge. These initial histories will be compared to the converged histories to determine whether or not they provide a good initial guess for the estimation method.

For both sets of data the $\mu$ initial time history was derived from the $\dot{x}_5$ state equation, again using a discrete time central difference to represent the derivative such that

$$\mu(t_i) = \sin^{-1}\left[ w\cos(\gamma(t_i))(x(t_{i+1}) - x(t_{i-1}))/((t_{i+1} - t_{i-1}) q C_L t_i \rho t_i s \nu(t_i)) \right] \qquad (20)$$

Note that $\gamma$, $\chi$, and $v$ represent flight path angle, azimuth, and magnitude of the velocity, respectively, as did $x_6$, $x_5$, and $x_4$ in the $\dot{x}_5$ equation.

Presently, $\beta$ is made up of three [nx1] vectors $C_L$, $C_D$, and $\mu$ (as mentioned previously, n is the number of data points for each of $C_L$, $C_D$, and $\nu$), hence, $\beta$ is a [3nx1] vector. Since the performance index is numerically differentiated with respect to each element of $\beta$, a smaller number of elements of $\beta$ will greatly reduce computation time. Because n is the time interval length divided by the time increment size, if n is small then either the increment

17

size is large or the interval length is short.   Since it
is desired to fit the data points to a smooth "true" function
of the parameters, a relatively short increment size is re-
quired whether the interval is long or short.   Therefore, the
size of n is predominately dependent upon the length of the
interval.   To reduce the computational load by decreasing
the size of n would then mean a short interval.   This would
lead to patching short intervals together in order to obtain
good parameter histories for a reasonable length of time.

To make n as large as possible and still cut down on
the length of $\beta$ , a Least Squares polynomial fit is made to
the $C_L$, $C_D$, and $\mu$ histories.   Since the true $C_L$, $C_D$, and $\mu$
time histories will be continuous functions of time, a
Least Squares polynomial fit to the discrete time parameter
data points is a reasonable model for their true histories.
The resulting coefficients are used as $\beta$ and are called upon
to calculate $C_L$, $C_D$, and $\mu$ , at any given time, for use in
the state equations.

A programming decision must be made when deciding the
order for the polynomials.   Reducing the size of $\beta$ without
sacrificing interval length was the initiative for using a
Least Squares polynomial model of the parameters, therefore
it is desired to fit the interval with the smallest order
polynomial, thereby decreasing the length of $\beta$ , and yet
maintain an accurate functional model of the parameter
histories.   A rough plot of the initial parameter histories

18

will give an idea what order polynomial will best approximate the true parameters. Thus, within this chapter the methodology for identifying parameters is explained as a weighted least squares minimization process. The Square-Root Variable-Metric algorithm, used in this report, minimizes the performance index, J, by a modified DFP optimization technique which is quasi second-order with respect to the parameters of interest ($\beta$). The derivative of J with respect to $\beta$ is calculated numerically using the central difference formula. The state equation model of the three DOF motion of the Space Shuttle was a flat Earth approximation. The experimental state histories were extracted from the radar data according to the coordinate system used. The initial parameter histories were derived from the equation of motion in the vertical direction (for $C_L$), Reference 1 (for $C_D$), and the $\dot{x}_5$ state equation (for $\mu$). Finally, the method of least squares was used to fit polynomials to the parameter histories, and the length of the $\beta$ vector was reduced by using the coefficients of these polynomials as $\beta$.

# III  Programming Considerations

After fitting the appropriate polynomials to the
guessed parameter histories, as was discussed in Chapter II,
the algorithm is ready to find the optimal $\beta$ .  This
chapter will expand upon some of the more delicate program-
ming characteristics of the algorithm.

## One Dimensional Search

The one dimensional search finds the value of $\alpha$  that
minimizes J in the $-HJ^T$ direction.

$$\min J(\beta + \triangle\beta)$$

(21)

where

$$\triangle\beta = -\alpha \, HJ^T$$

Note that it is this $-HJ^T$ that supplies the algorithm with
quasi second-order convergence characteristics, since as H
is updated it approaches the inverse of the Hessian matrix.
There are many methods for arriving at the correct $\alpha$  but
all methods have certain inherent problems.  The algorithm
becomes very sensitive to very small changes in $\beta$  as
convergence is approached.  Therefore, it is important to

keep from choosing a $\beta$ that give a value for J too far

beyond the minimum in the $-HJ^T$ direction since even a

small $\Delta\beta$ added to the $\beta$ can cause great changes in

J. This could result in improper updating of the S matrix

and likewise lead to searches in the wrong direction on

following iterations.

The method used to calculate $\Delta\beta$ in this report

(Ref 2) involved setting $\alpha_i$ equal to $\alpha_{i-1} + \xi$ , where

i=1,2,...; and $\alpha_0$ , the initial $\alpha$ , is 0., and $\xi$

is a small constant of magnitude less than 0.1. This

new $\alpha_i$ is used to calculate $\beta_i = \beta_{i-1} + \Delta\beta_i$ ,

and, hence, $J_i(\beta_i)$. This $J_i(\beta_i)$ is compared to

$J_{i-1}(\beta_{i-1})$ . If $J_i$ is less than $J_{i-1}$, several

decisions must be made before the minimizing $\alpha$ can

be found. If the difference between $J_i$ and $J_{i-1}$ is less

than some tolerance, then $J_{-1}$ can be considered the

minimum. If the difference is greater than this

tolerance, the size of $\xi$ is decreased and the

search is restarted from $J_{i-1}$. This procedure of decreasing

$\xi$ and restarting the search continues until $(J_{i-1} -$

$J_i)/J_{i-1}$ is less than the required tolerance. Note that

$\alpha$ must indicate the sum of all initialized and reinitial-

ized step sizes. Also, since it will remain positive

definite, the tolerances need not be extremely small to

maintain good convergence of the algorithm.

## Convergence Criteria

The convergence criterion is based on $(J_O - J_{(i-1)})/J_O$
less than some tolerance, where $J_O$ and $J_{i-1}$ are minimum
values of the performance index from two successive search
directions. If $(J_O - J_{(i-1)})/J_O$ is less than the prescribed
tolerance, and, likewise, $A \longrightarrow O$, $B \longrightarrow O$, and $\propto \longrightarrow 1$, then
the algorithm has converged. As convergence is approached,
the minimum J, $J_{(i-1)}$, may be the same as the value of $J_O$ if
the one dimensional search only takes one step before its
tolerance is satisfied. For this case, if the percentage
difference $(J_O - J_{(i-1)})/J_O$ is greater than the prescribed
tolerance, then this tolerance, and the tolerance for the
one dimensional search are decreased and the one-dimensional
search is restarted. If the percentage difference is less
than the prescribed tolerance, and A, B, and $\propto$ have not
converged, then the S matrix is reinitialized to the identity
matrix, I, and a gradient step is taken. This is done on
the chance that H is not converging to the inverse Hessian
matrix and needs to be reinitialized. Generally, the
algorithm has reached convergence before this step is used.

## Differentiation

Another programming consideration is the choice of the
best $\in$ for the numerical differention of $J(\beta)$. Hull

22

and Williamson (Ref 4) explain a method for calculating the best $\epsilon$ which involves taking second numerical derivatives. Instead, to simplify the algorithm further, derivatives were calculated with several different values of $\epsilon$ . A value of $\epsilon = 1.0E-4$ gave the largest number of significant digits in the derivative without it being affected by computer roundoff, making this the $\epsilon$ of choice for this algorithm.

## Nondimensional Coefficients

For higher order polynomials, such as the sixth order polynomial used to fit the parameter histories, the relative magnitude between coefficients may be very large. Since these coefficients are all differentiated using the same size $\epsilon$ , the elements of the J vector may likewise be of widely varying magnitudes. This makes the algorithm more sensitive to some elements than others, thereby retarding the overall update of S. Also, this disparity in J element magnitude will increase the truncation error, hence, weakening the ability of the algorithm to converge.

This algorithm therefore used a nondimensional $\beta$ vector to make the magnitudes of the polynomial coefficients more "even", thereby making the $J_\beta$ elements about the same order of magnitude also. This involved multiplying the coefficients by the final time of the interval to the

power that the coefficient has in the polynomial (for instance, a second order polynomial, $C_o + C_1 t + C_2 t^2$, would have $C_o$, $C_1 t_f$ and $C_2 t_f^2$ as the nondimensional coefficients). These elements of $\beta$ had to be redimensionalized, by dividing by the appropriate power of $t_f$, before calculating the $C_L(t_i)$, $C_D(t_i)$, and $\mu(t_i)$ values called for in the state equations during the integration.

## Weighting Matrix

The weighting matrix had to be adjusted to find the best choice of diagonal elements for the fastest convergence. The Multisensor Report gives an idea of the uncertainties to expect of radar data (Ref 8) as shown in the Appendix. The use of a diagonal weighting matrix is a restriction to the full inverse measurement covariance matrix weighting. Although the statistical description of the radar data state errors are correlated, a diagonal, uncorrelated, error model was used to simplify the computations, and hence, speed the convergence of the algorithm. The fastest convergence was achieved by weighting the values of $x_5$ and $x_6$ (angles) up to eight orders of magnitude more than the $x_1$, $x_2$, and $x_3$ (distances) states, and up to four orders of magnitude more than $x_4$ (velocity). Comparisons are made in Chapter IV of runs using different weights.

## IV Results

Two runs were made, using Multisensor Report data, to test the convergence characteristics of the algorithm. Once the algorithm was working properly, a run using BET data was fully converged and analyzed. The two test runs, (call them Run 1 and Run 2), were straight landing approaches. Therefore the $\dot{x}_5$ equation (rate of change of azimuth) was nearly zero, implying very small bank angles. The BET data was taken from a turn. This arrangement of data runs allowed evaluation of the algorithm characteristics during a relatively simple flight history before testing the performance of the algorithm during a period of active maneuvering.

### Run 1

The first run spanned a seventy-eight second time interval, ranging in altitude from 8667.5 feet to 14.9 feet. Table 1 lists the calculated versus experimental state histories, and the difference between them, element by element. This run used 500 seconds of Central Processor (CP) time to converge to $A = 9.2$ $E - 6$, $B = 3.6$ $E - 5$, and $\alpha = 1$ using sixth order polynomials to fit the parameter histories. The converged parameter histories are shown in Figures 5, 6, and 7 along with the initial parameter histories. These figures display the effectiveness of the method used to calculate the initial parameters. The curves show corresponding peaks and valleys and are of the same order, which

# Table I

## State Histories (Run 1)

| Time (sec) | $x_1$ of G / $x_1$ of Y / $x_1$-DIFF (ft) | $x_2$ of G / $x_2$ of Y / $x_2$-DIFF (ft) | $x_3$ of G / $x_3$ of Y / $x_3$-DIFF (ft) | $x_4$ of G / $x_4$ of Y / $x_4$-DIFF (ft/sec) | $x_5$ of G / $x_5$ of Y / $x_5$-DIFF (rad) | $x_6$ of G / $x_6$ of Y / $x_6$-DIFF (rad) |
|---|---|---|---|---|---|---|
| 6.0 | 25154.3 | 12182.7 | 8049.5 | 582.2 | 4.26021 | -.352506 |
|  | 25114.3 | 12285.1 | 8085.3 | 575.7 | 4.2481 | -.34208 |
|  | -40. | 102.4 | 36.8 | -6.5 | -.01211 | .010526 |
| 18.0 | 19323.5 | 9539.4 | 5724.3 | 552.9 | 4.29792 | -.345674 |
|  | 19219.4 | 9652.1 | 5688.8 | 562. | 4.2603 | -.35954 |
|  | -104.1 | 112.7 | -35.5 | 9.1 | -.03762 | -.013866 |
| 30.0 | 13737.8 | 6967.9 | 3504.7 | 541.5 | 4.25736 | -.343423 |
|  | 13415.6 | 6982.5 | 3533.5 | 531.8 | 4.2324 | -.32987 |
|  | -322.2 | 14.6 | 28.8 | -9.7 | -.02496 | .013553 |
| 42.0 | 8231.2 | 4137.8 | 1482. | 542.6 | 4.22642 | -.269352 |
|  | 7978.5 | 4112.8 | 1336.6 | 543.6 | 4.281 | -.33685 |
|  | -252.7 | -25. | -145.4 | 1. | -.02542 | -.067499 |
| 54.0 | 2710.5 | 1279.8 | 282.5 | 502.7 | 4.25053 | -.102491 |
|  | 2400.7 | 1182.3 | 142.2 | 500.6 | 4.2726 | -.04538 |
|  | -309.8 | -97.5 | -140.3 | -2.1 | .02207 | .057111 |
| 66.0 | -2228.9 | -1074. | 74.5 | 405.4 | 4.2807 | .003491 |
|  | -2527.5 | -1180.2 | 45.4 | 402.7 | 4.2638 | -.01047 |
|  | -298.6 | -105.2 | -29.1 | -2.7 | -.0169 | -.013961 |
| 78.0 | -6143. | -2892.5 | 55.3 | 321.8 | 4.26536 | -.038138 |
|  | -6448.9 | -3066.7 | 14.9 | 320.8 | 4.2726 | -.00524 |
|  | -305.9 | -174.2 | -40.4 | -1. | .00724 | .002898 |

DIFF = Difference between $x_i$ of Y and $x_i$ of G

26
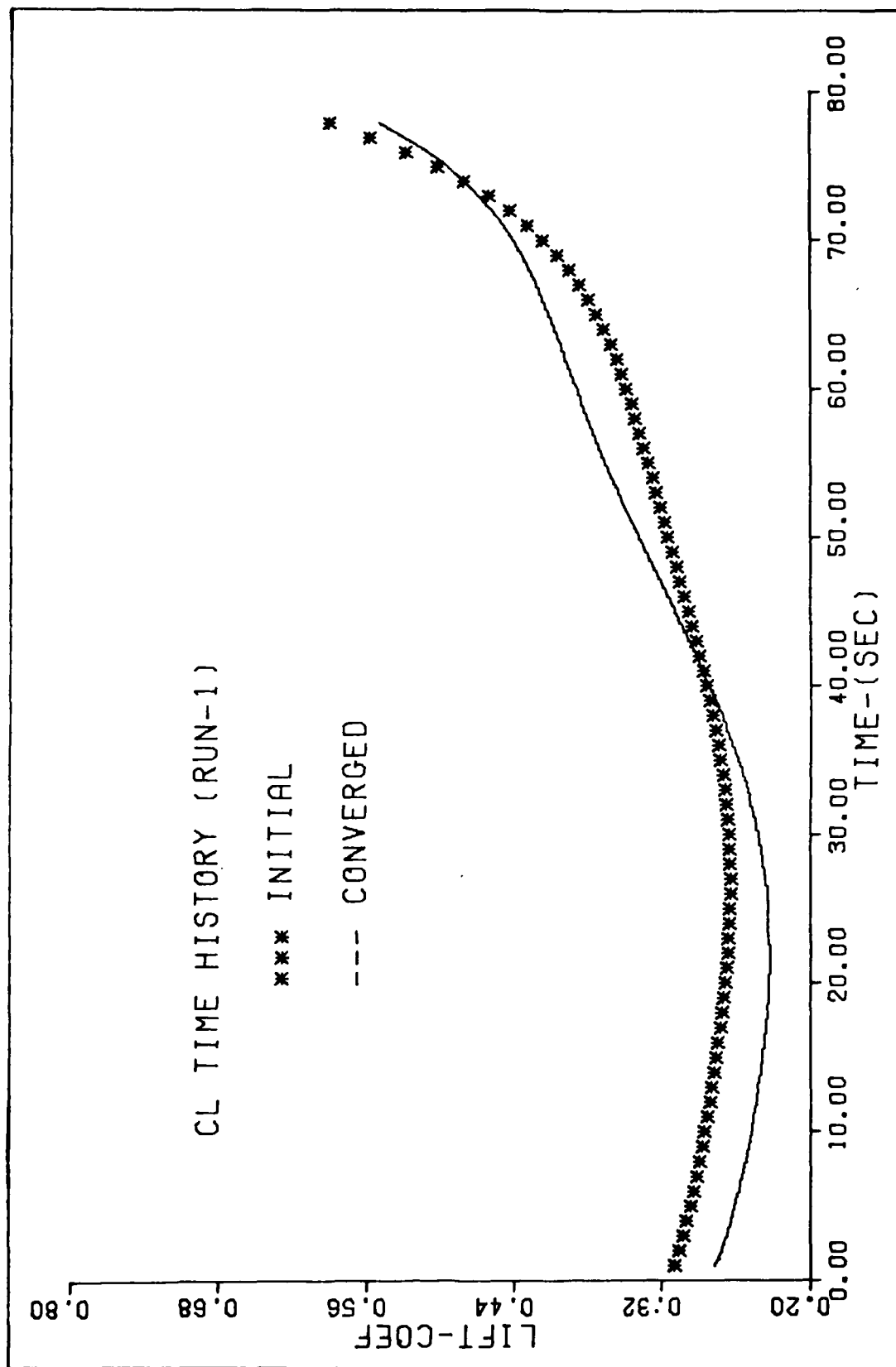
Fig. 5. Initial and Converged $C_L$ (Run 1)
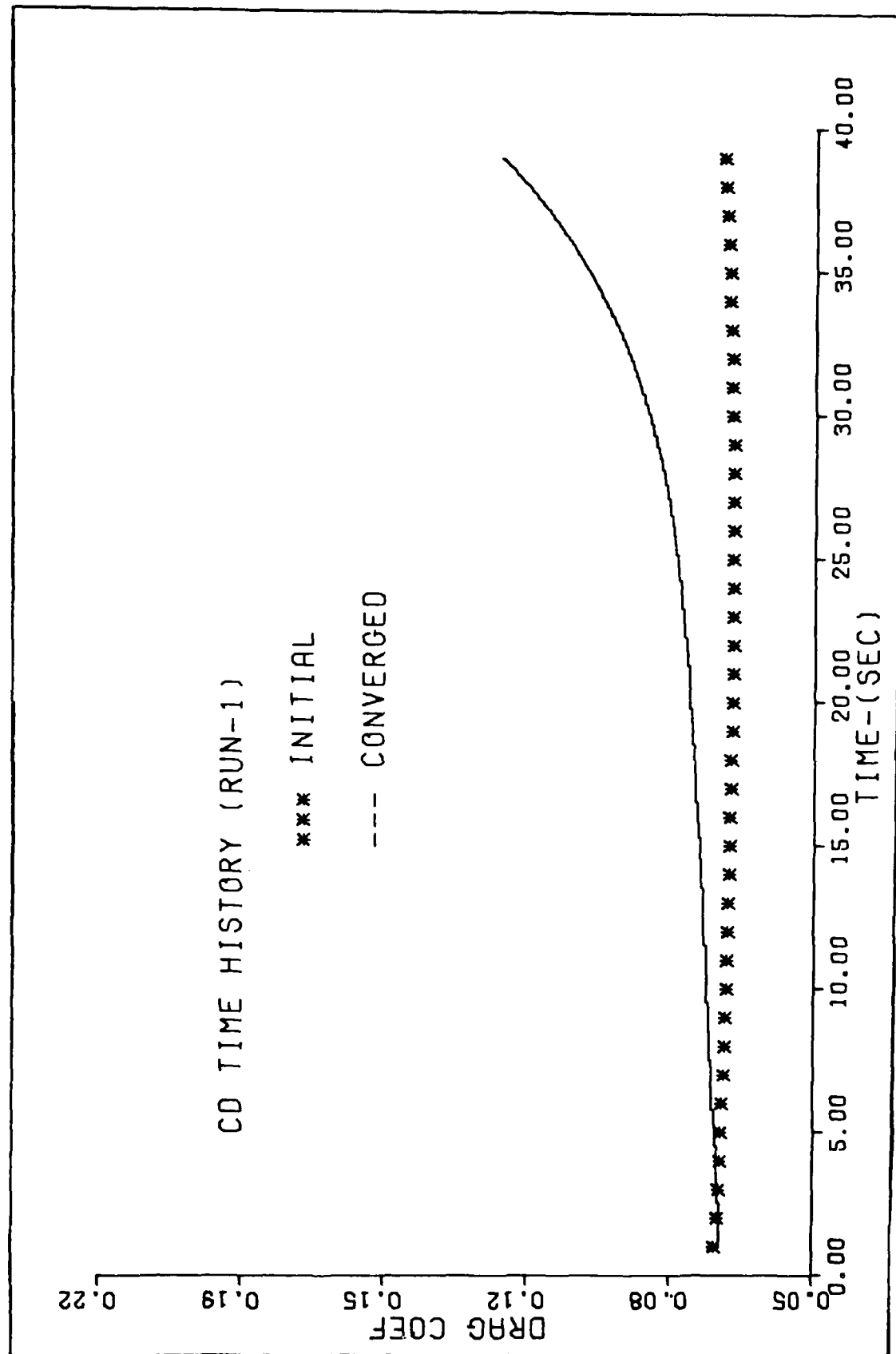
Fig. 6. Initial and Converged $C_D$ (Run 1)

28
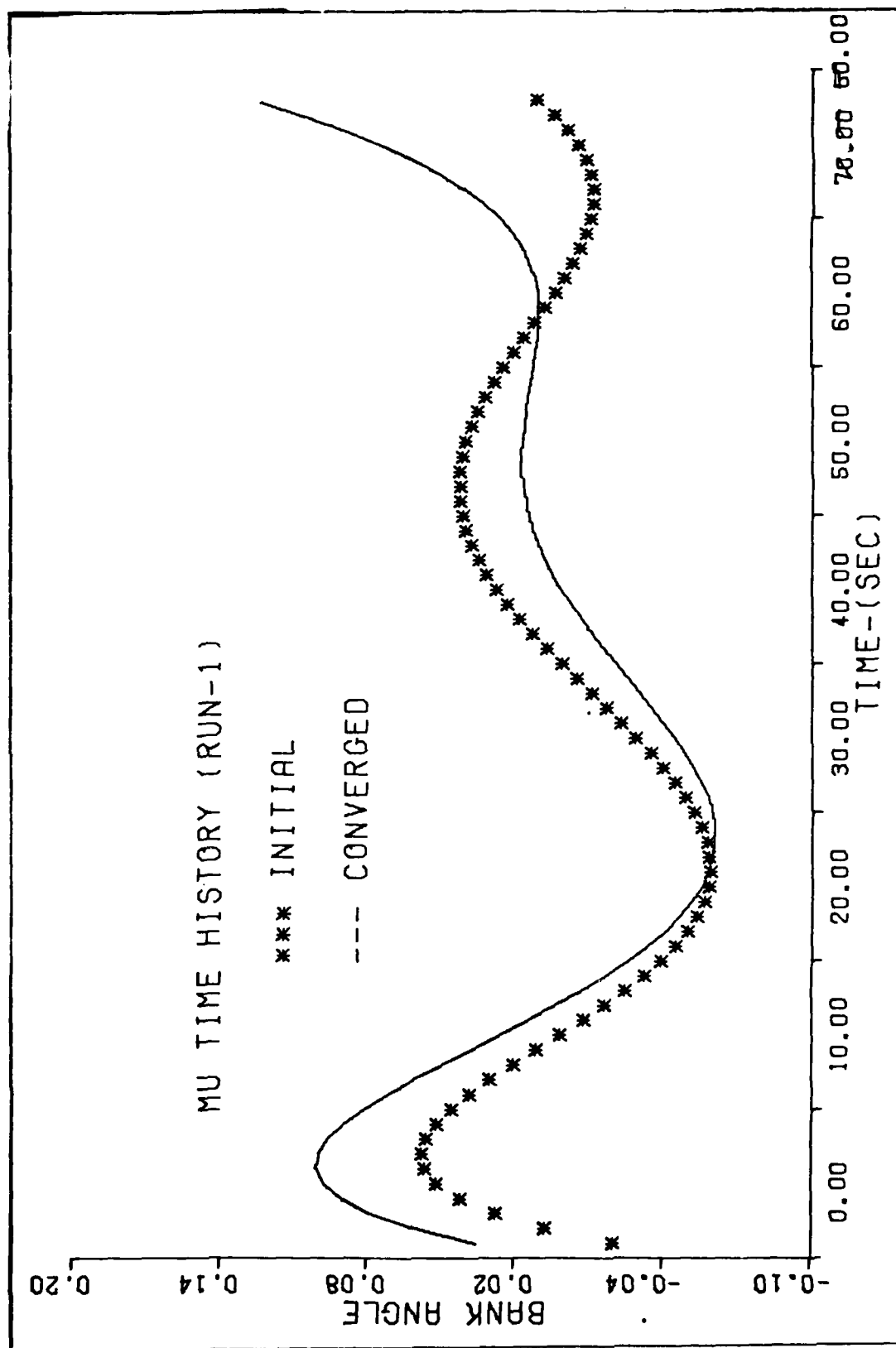
Fig. 7. Initial and Converged $\mu$ (Run 1)

means the initial parameter histories did not require extensive changes, implying fast convergence. Although the magnitudes differ somewhat for $C_L$ and $C_D$, this can be attributed to the inaccuracy of the reference area $s$ $(2960 \text{ ft}^2)$ and the average value used for w (198,200 lb), which were used in calculating the initial parameters. The accuracy of the algorithm for this run is on the order of 100 ft for the $x_1$, $x_2$, and $x_3$ states, 5 ft/sec for $x_4$, and 0.02 rad for states $x_5$ and $x_6$ (Table I).

Run 2

The second run spanned the first thirty-nine seconds of Run 1 and used 500 CP seconds to converge to A = 5.2 E - 9, B = 7.9 E - 9, and $\propto$ = 1. The order of the polynomial used to fit the parameter histories was varied from second to sixth order. Figure 8 shows the converged lift coefficient histories for the two extreme cases of second order and sixth order. The second order $C_L$ curve slices through the hills and valleys of the sixth order curve, yet, as Tables II and III show, the state history fits for both runs are nearly the same. This illustrates the importance of choosing a polynomial of large enough order such that all of the gross characteristics of the true parameter history are mapped.

This interval was also used as a comparison to Run 1 to study how choice of interval length and order of poly-
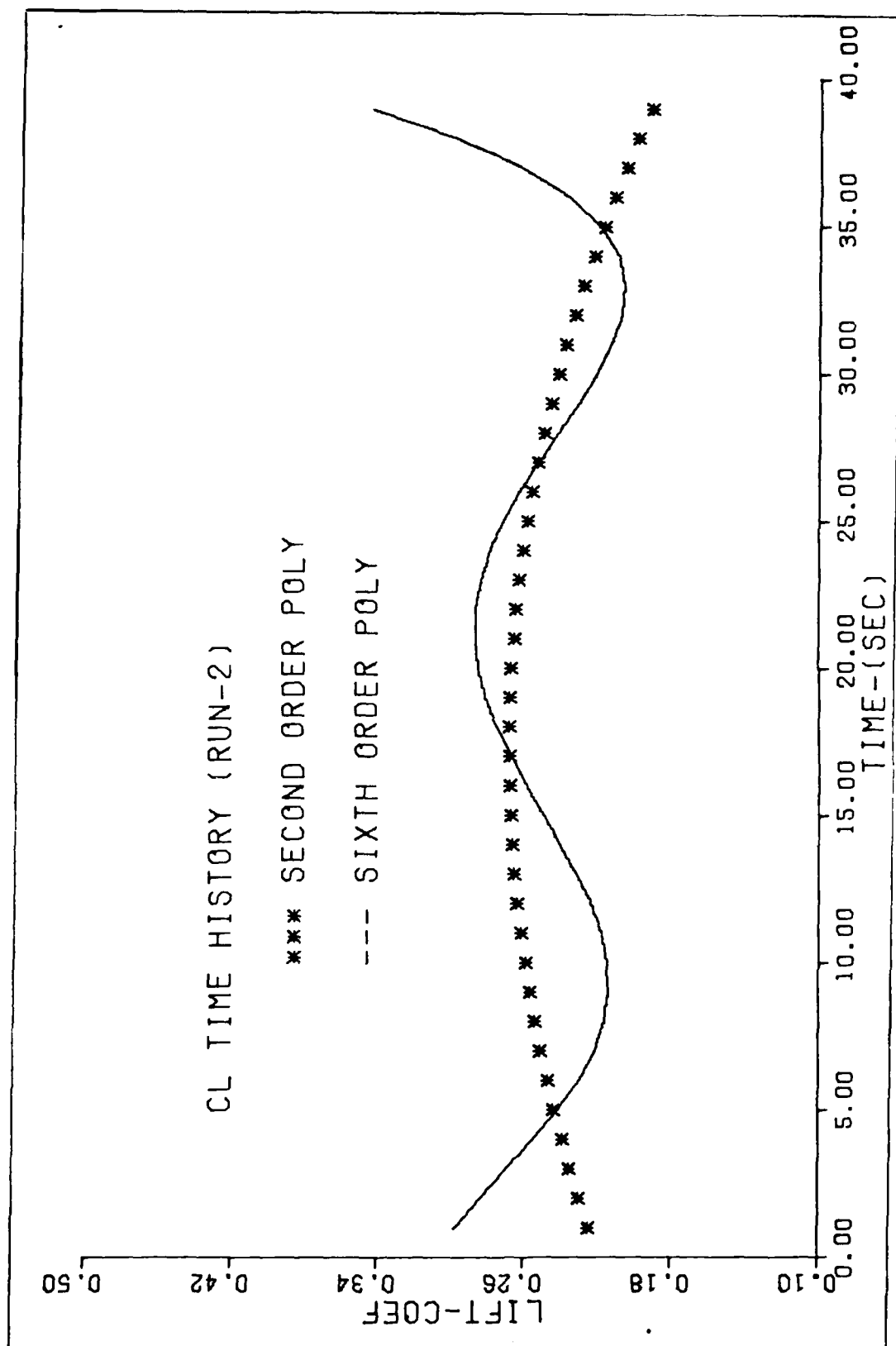
Fig. 8. $C_L$ for Sixth vs. Second Order Polynomials (Run 2)

Table II

Second Order Polynomial State Histories (Run 2)

| Time (sec) | $x_1$ of G $x_1$ of Y $x_1$-DIFF (ft) | $x_2$ of G $x_2$ of Y $x_2$-DIFF (ft) | $x_3$ of G $x_3$ of Y $x_3$-DIFF (ft) | $x_4$ of G $x_4$ of Y $x_4$-DIFF (ft/sec) | $x_5$ of G $x_5$ of Y $x_5$-DIFF (rad) | $x_6$ of G $x_6$ of Y $x_6$-DIFF (rad) |
|---|---|---|---|---|---|---|
| 3.0 | 26636.5 26603.4 -33.1 | 12931.6 12965.6 34. | 8648.4 8667.5 19.1 | 580.1 582.5 2.4 | 4.25241 4.2394 -.01301 | -.366667 -.34208 .024587 |
| 9.0 | 23732.2 23532.4 -99.8 | 11551. 11621.9 70.9 | 7400.4 7504.6 104.2 | 570.4 565.3 -5.1 | 4.2816 4.2569 -.0247 | -.368668 -.35605 .012618 |
| 15.0 | 20834.5 20593.1 -141.4 | 10240.7 10312.7 72. | 6204.2 6291. 86.8 | 562.1 560.4 -1.7 | 4.29054 4.2638 -.02674 | -.348519 -.37001 -.021391 |
| 21.0 | 17958.4 17747.8 -210.6 | 8938.8 8986.9 48.1 | 5100.8 5108.9 8.1 | 552.5 558.9 6.4 | 4.28144 4.2534 -.02804 | -.324626 -.34208 -.017454 |
| 27.0 | 15137.1 14830.2 -306.9 | 7606.9 7656. 49.1 | 4075.3 4045.3 -30. | 542.4 540.5 -1.9 | 4.25957 4.2603 .00073 | -.313999 -.32114 -.007141 |
| 33.0 | 12398.9 12038.7 -359.2 | 6227.8 6282.2 54.4 | 3061.4 3009.4 -52. | 534.8 529.6 -5.2 | 4.23146 4.2185 -.01296 | -.330014 -.34208 -.012066 |
| 39.0 | 9754.7 9328.2 -426.5 | 4799.2 4862.2 62.3 | 1957.1 1899.9 -57.2 | 534. 538.8 4.8 | 4.2035 4.2045 .001 | -.380419 -.3577 .022719 |

DIFF = Difference between $x_i$ of Y and $x_i$ of G

32

Table III

## Sixth Order Polynomial State Histories (Run 2)

| Time (sec) | x of G / x of Y / x -DIFF (ft) | x of G / x of Y / x -DIFF (ft) | x of G / x of Y / x -DIFF (ft) | x of G / x of Y / x -DIFF (ft/sec) | x of G / x of Y / x -DIFF (rad) | x of G / x of Y / x -DIFF (rad) |
|---|---|---|---|---|---|---|
| 3.0 | 26636.5 | 12931.6 | 8648.4 | 580.1 | 4.25241 | -.366667 |
|  | 26603.4 | 12965.6 | 8667.5 | 582.5 | 4.2394 | -.34208 |
|  | -33.1 | 34. | 19.1 | 2.4 | -.01301 | .024587 |
| 9.0 | 23732.2 | 11551. | 7400.4 | 570.4 | 4.2815 | -.358668 |
|  | 23603.4 | 11621.9 | 7504.5 | 565.3 | 4.2569 | -.35605 |
|  | -99.8 | 70.9 | 104.2 | -5.1 | -.0247 | .012618 |
| 15.0 | 20834.5 | 10240.7 | 6204.2 | 562.1 | 4.29054 | -.348619 |
|  | 20693.1 | 10312.7 | 6291. | 560.4 | 4.2638 | -.37001 |
|  | -141.4 | 72. | 86.8 | -1.7 | -.02674 | -.021391 |
| 21.0 | 17958.4 | 8938.8 | 5100.8 | 552.5 | 4.28144 | -.324627 |
|  | 17747.8 | 8985.9 | 5108.9 | 558.9 | 4.2534 | -.34208 |
|  | -210.6 | 48.1 | 8.1 | 6.4 | -.02804 | -.017453 |
| 27.0 | 15137.1 | 7605.9 | 4075.3 | 542.4 | 4.35957 | -.314 |
|  | 14830.2 | 7656. | 4045.3 | 540.5 | 4.2603 | -.32114 |
|  | -306.9 | 49.1 | -30. | -1.9 | .00073 | -.00714 |
| 33.0 | 12398.9 | 6227.8 | 3061.4 | 534.8 | 4.23146 | -.330014 |
|  | 12039.7 | 6282.2 | 3009.4 | 529.6 | 4.2185 | -.34208 |
|  | -359.2 | 54.4 | -52. | -5.2 | -.01296 | -.012066 |
| 39.0 | 9754.7 | 4799.9 | 1957.1 | 534. | 4.2035 | -.380419 |
|  | 9328.2 | 4862.2 | 1899.9 | 538.8 | 4.2045 | -.3577 |
|  | -426.5 | 62.3 | -57.2 | 4.8 | .001 | .022719 |

DIFF = Difference between $x_i$ of Y and $x_i$ of G

nomial affects the accuracy and convergence of the algorithm.
A comparison of Tables I and II, both calculated using
sixth order polynomials, shows that Run 2 was only slightly
more accurate than Run 1 at fitting the experimental state
histories over the same time intervals. Yet, comparing
Figures 9, 10, and 11 to the Run 1 figures shows that the
true parameter histories are more fully described by Run 2.
Therefore, the appropriate length of the interval and the
polynomial order are very dependent upon each other for
properly describing the true parameter  histories.  Again,
the initial parameter histories give a good means for
choosing an appropriate polynomial order.

This interval was also used to test the effect of
different W diagonal elements.  Tables IV-VI represent
three state histories, each with a different W.  Table IV
uses 1.E4 for the first three diagonal elements of W, (call
them w1, w2, w3, respectively), 1. for w4, 1.E-4 for w5
and w6.  This represents very accurate radar measurements
for the $x_1$, $x_2$, and $x_3$ states relative to the measurements
for the $x_5$ and $x_6$ states.  Table V, $W_2$, is with all six
diagonal elements as 1, such that all six radar measurements
are assummed of equal accuracy.  Table III is the opposite
extreme to Table IV with, w1, w2, w3 as 1.E-8, w4 as 1.E-4,
w5 and w6 as 1.  Comparing the convergence characteristics
of the algorithm using these different weighting matrices

34
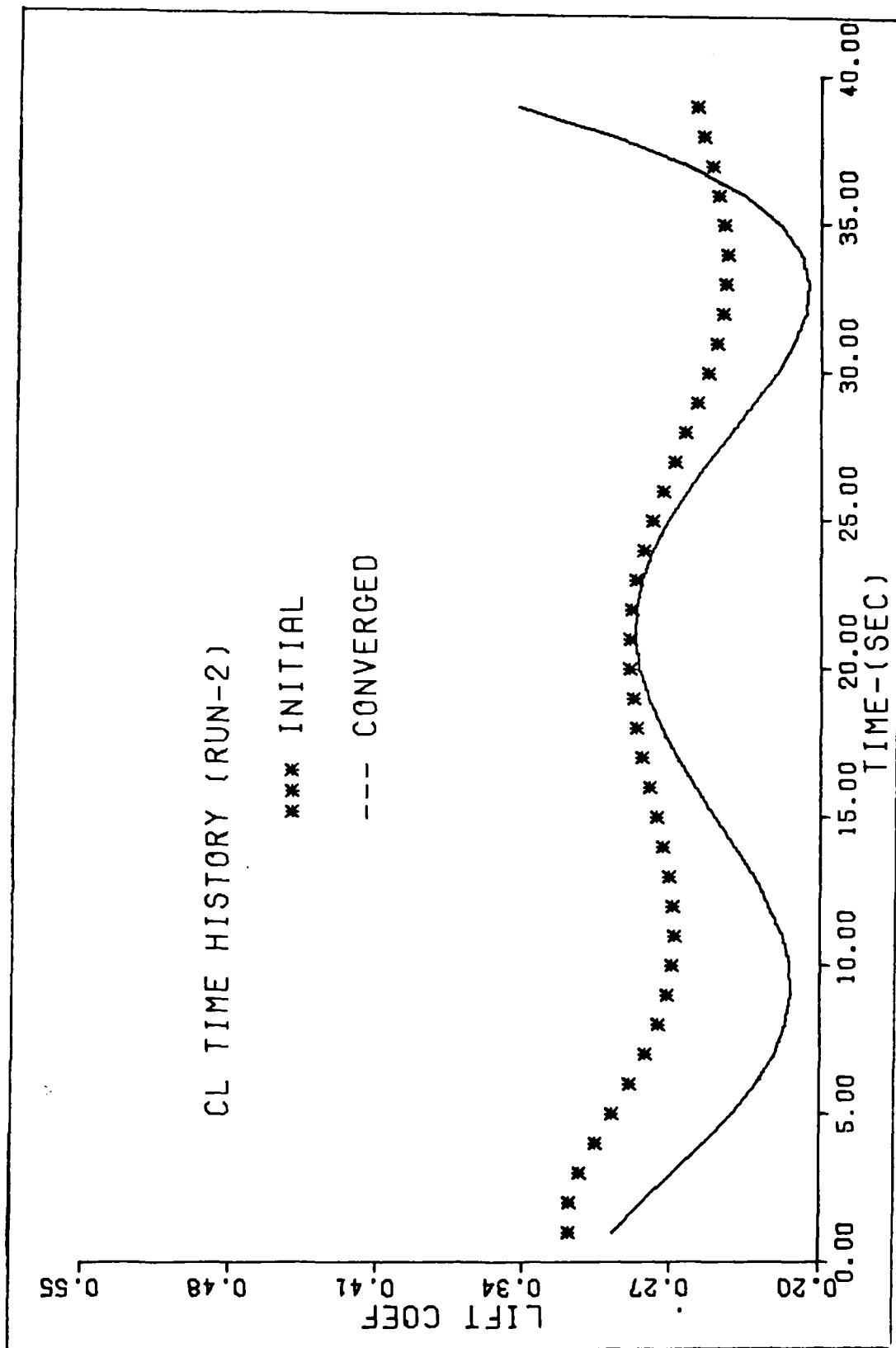
Fig. 9. Initial and Converged $C_L$ (Run 2)
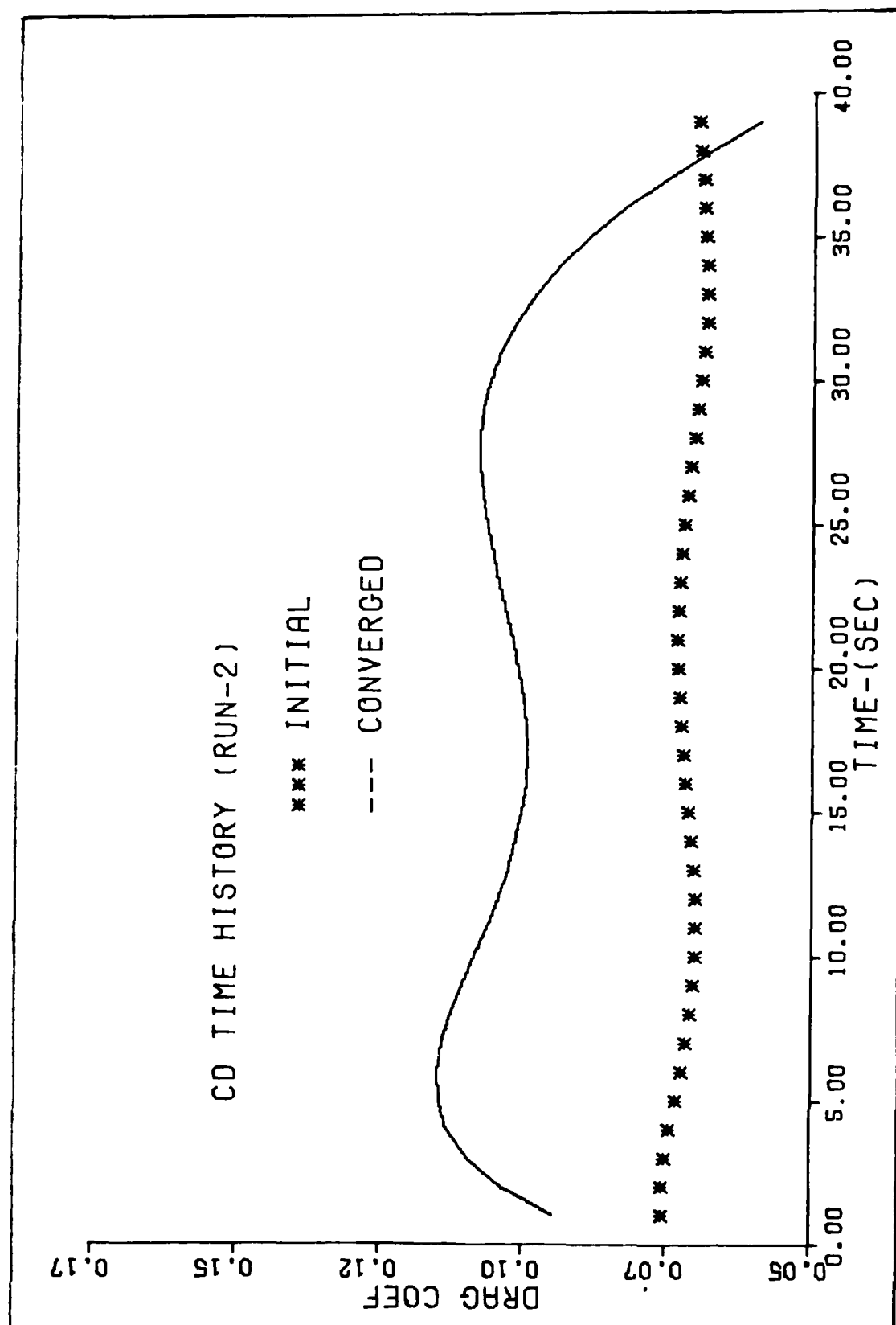
Fig. 10. Initial and Converged $C_D$ (Run 2)
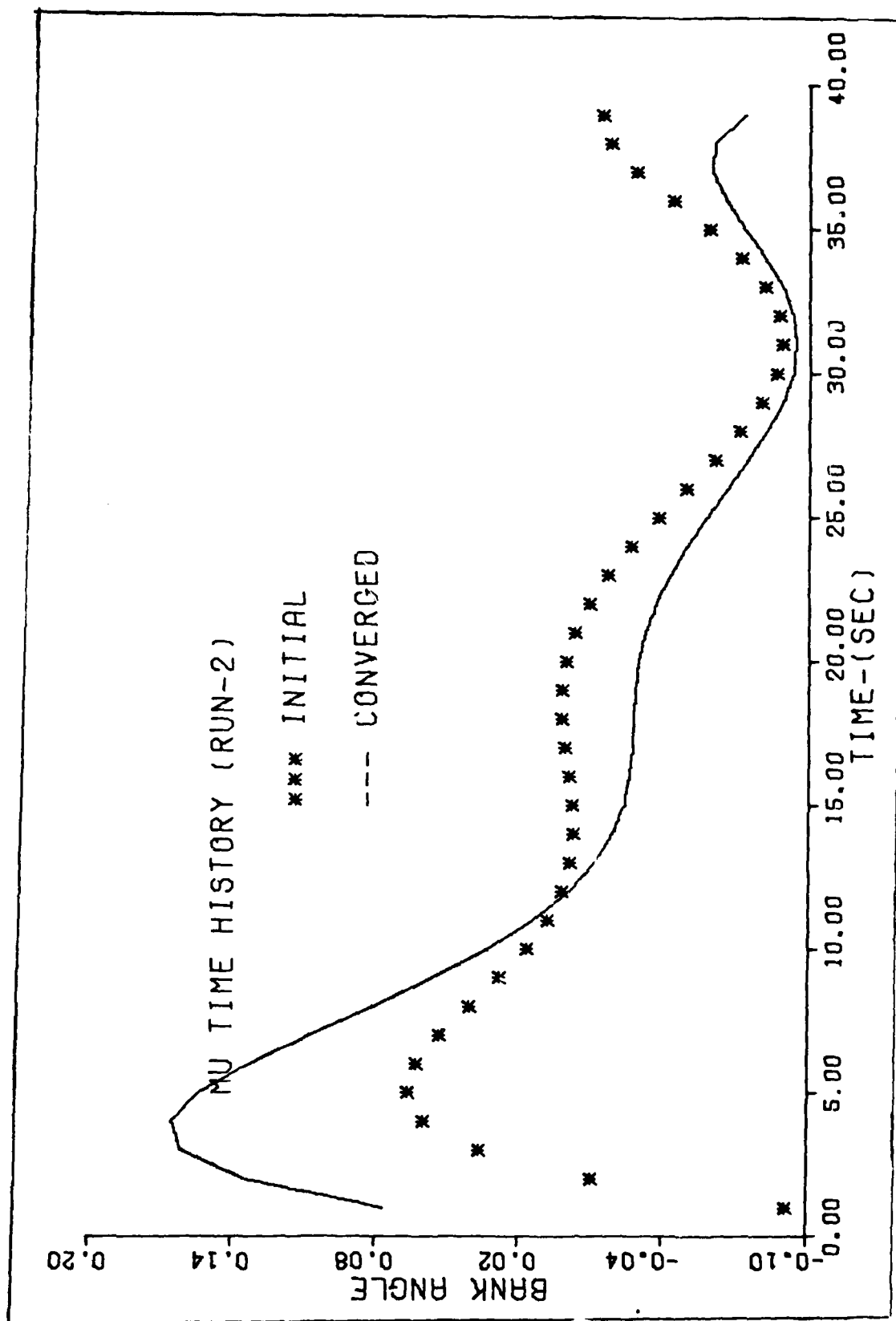
Fig. 11. Initial and Converged ∧ (Run 2)

Table IV

State Histories for W1 (Run 2)

| Time (sec) | $x_1$ of G<br>$x_1$ of Y<br>$x_1$-DIFF<br>(ft) | $x_2$ of G<br>$x_2$ of Y<br>$x_2$-DIFF<br>(ft) | $x_3$ of G<br>$x_3$ of Y<br>$x_3$-DIFF<br>(ft) | $x_4$ of G<br>$x_4$ of Y<br>$x_4$-DIFF<br>(ft/sec) | $x_5$ of G<br>$x_5$ of Y<br>$x_5$-DIFF<br>(rad) | $x_6$ of G<br>$x_6$ of Y<br>$x_6$-DIFF<br>(rad) |
|---|---|---|---|---|---|---|
| 3.0 | 26607.2<br>26603.4<br>-3.8 | 12938.7<br>12965.6<br>25.9 | 8678.1<br>8667.5<br>-10.6 | 584.9<br>582.5<br>-2.4 | 4.27907<br>4.2394<br>-.03967 | -.330665<br>-.34208<br>-.011415 |
| 9.0 | 23606.9<br>23632.4<br>25.5 | 11641.5<br>11621.9<br>-19.6 | 7553.5<br>7504.5<br>-48.9 | 569.6<br>565.3<br>-4.3 | 4.30936<br>4.2569<br>-.05246 | -.344296<br>-.35605<br>-.01175 |
| 15.0 | 20683.5<br>20693.1<br>9.5 | 10348.<br>10312.7<br>-35.3 | 6331.5<br>6291.<br>-40.5 | 573.8<br>560.4<br>-13.4 | 4.28289<br>4.2638<br>-.01909 | -.378847<br>-.37001<br>.008837 |
| 21.0 | 17753.2<br>17747.8<br>-5.4 | 8994.8<br>8985.9<br>-7.9 | 5089.7<br>5108.9<br>19.2 | 575.7<br>558.9<br>-16.8 | 4.2808<br>4.2534<br>-.0274 | -.343946<br>-.34208<br>.001866 |
| 27.0 | 14822.3<br>14830.2<br>7.9 | 7636.7<br>7655.<br>19.3 | 4032.2<br>4045.3<br>13.1 | 554.2<br>540.5<br>-13.7 | 4.27064<br>4.2603<br>-.01034 | -.298867<br>-.32114<br>-.022273 |
| 33.0 | 12044.3<br>12039.7<br>-4.6 | 6283.<br>6282.2<br>-.8 | 3017.5<br>3009.4<br>-8.1 | 534.3<br>529.6<br>-4.7 | 4.24955<br>4.2185<br>-.03105 | -.350458<br>-.34208<br>.008378 |
| 39.0 | 9368.6<br>9328.2<br>-40.4 | 4848.3<br>4862.2<br>13.9 | 1915.1<br>1899.<br>-15.2 | 548.4<br>538.8<br>-9.6 | 4.1116<br>4.2045<br>.0929 | -.283106<br>-.3577<br>-.074594 |

DIFF = Difference between $x_i$ of Y and $x_i$ of G

Table V

State Histories for W2 (Run 2)

| Time (sec) | $x_1$ of G / $x_1$ of Y / $x_1$-DIFF (ft) | $x_2$ of G / $x_2$ of Y / $x_2$-DIFF (ft) | $x_3$ of G / $x_3$ of Y / $x_3$-DIFF (ft) | $x_4$ of G / $x_4$ of Y / $x_4$-DIFF (ft/sec) | $x_5$ of G / $x_5$ of Y / $x_5$-DIFF (rad) | $x_6$ of G / $x_6$ of Y / $x_6$-DIFF (rad) |
|---|---|---|---|---|---|---|
| 3.0 | 26580.7 | 12925.6 | 8658.1 | 507.9 | 4.27551 | -.338229 |
|  | 26603.4 | 12965.6 | 8667.5 | 582.5 | 4.2394 | -.34208 |
|  | 22.7 | 40. | 9.4 | -15.4 | -.03611 | -.003851 |
| 9.0 | 23604.9 | 11615.6 | 7509.5 | 558.1 | 4.30572 | -.350588 |
|  | 23632.4 | 11621.9 | 7504.6 | 565.3 | 4.2569 | -.35605 |
|  | 27.5 | 6.3 | -4.9 | 7.2 | -.04882 | -.005462 |
| 15.0 | 20716.3 | 10343.6 | 6309.9 | 573.8 | 4.28822 | -.357958 |
|  | 20693.1 | 10312.7 | 6291. | 560.4 | 4.2638 | -.37001 |
|  | -23.2 | -30.9 | -18.9 | -13.4 | -.02442 | -.002052 |
| 21.0 | 17741.3 | 8985.2 | 5102.9 | 580. | 4.28332 | -.333341 |
|  | 17747.8 | 8985.9 | 5108.9 | 558.9 | 4.3534 | -.34208 |
|  | 6.5 | 1.7 | 6. | -21.1 | -.02992 | -.008739 |
| 27.0 | 14819.2 | 7644.1 | 4045.5 | 546.6 | 4.27632 | -.311222 |
|  | 14830.2 | 7655. | 4045.3 | 540.5 | 4.2603 | -.32114 |
|  | 11. | 11.9 | -.2 | -6.1 | -.01602 | -.009858 |
| 33.0 | 12056.2 | 6298.9 | 3010.7 | 544.1 | 4.23853 | -.342631 |
|  | 12039.7 | 6282.2 | 3009.4 | 529.6 | 4.2185 | -.34208 |
|  | -16.5 | -16.7 | -1.3 | -14.5 | -.02003 | -.000551 |
| 39.0 | 9325.3 | 4848.9 | 1905.2 | 522.9 | 4.22591 | -.322315 |
|  | 9328.2 | 4862.2 | 1899.9 | 538.8 | 4.2045 | -.3577 |
|  | 2.9 | 13.3 | -6.3 | 15.9 | -.02141 | -.035385 |

DIFF = Difference between $x_i$ of Y and $x_i$ of G

Table VI

State Histories (Run 3)

| Time (sec) | $x_1$ of G<br>$x_1$ of Y<br>$x_1$-DIFF<br>(ft) | $x_2$ of G<br>$x_2$ of Y<br>$x_2$-DIFF<br>(ft) | $x_3$ of G<br>$x_3$ of Y<br>$x_3$-DIFF<br>(ft) | $x_4$ of G<br>$x_4$ of Y<br>$x_4$-DIFF<br>(ft/sec) | $x_5$ of G<br>$x_5$ of Y<br>$x_5$-DIFF<br>(rad) | $x_6$ of G<br>$x_6$ of Y<br>$x_6$-DIFF<br>(rad) |
|---|---|---|---|---|---|---|
| 3.0 | -53292.5<br>-53262.6<br>29.8 | -6167.2<br>-6175.3<br>-8.1 | 17065.8<br>17064.7<br>-1.1 | 605.7<br>613.1<br>7.4 | -1.19648<br>-1.21249<br>-.016 | -.255783<br>-.250091<br>.006 |
| 12.0 | -49293.1<br>-49092.5<br>200.6 | -2820.2<br>-2987.3<br>-167. | 15593.5<br>15695.2<br>101.7 | 605.2<br>599.2<br>-5.9 | -1.46558<br>-1.47314<br>-.008 | -.297804<br>-.278401<br>.019 |
| 21.0 | -44526.7<br>-44438.9<br>87.8 | -856.4<br>-872.7<br>-16.3 | 13870.4<br>13913.3<br>42.8 | 606.2<br>609.9<br>3.7 | -1.76756<br>-1.67224<br>.095 | -.341253<br>-.381764<br>-.041 |
| 30.0 | -39500.2<br>-39482.7<br>17.4 | -32.9<br>102.3<br>135.1 | 11957.9<br>11881.5<br>-76.3 | 603.5<br>602.9<br>-.6 | -1.91483<br>-1.09473<br>.01 | -.388649<br>-.381707<br>-.004 |
| 39.0 | -34513.3<br>-34461.1<br>52.1 | 299.2<br>230.7<br>-68.5 | 9915.7<br>9999.<br>82.3 | 594.5<br>592.1<br>-2.4 | -1.98017<br>-1.99489<br>-.015 | -.385838<br>-.359206<br>.017 |
| 48.0 | -29584.3<br>-29512.6<br>71.7 | 375.4<br>256.9<br>-118.5 | 8058.8<br>8217.4<br>158.5 | 576.2<br>578.<br>1.8 | -2.00653<br>-1.97712<br>.029 | -.332453<br>-.351077<br>-.019 |
| 57.0 | -24736.1<br>-24670.<br>66.1 | 510.8<br>385.1<br>-125.7 | 6301.3<br>6461.3<br>160.4 | 575.5<br>573.2<br>-2.3 | -1.98293<br>-1.9584<br>-.002 | -.410185<br>-.376647<br>.034 |

DIFF = Difference between $x_i$ of Y and $x_i$ of G

provides a method for choosing the best weighting matrix.

As would be expected, the heavily weighted states converged better for all three cases. Table V shows that the algorithm ignores the small $x_5$ and $x_6$ histories because they contribute little to the performance index compared to the $x_1$, $x_2$, and $x_3$ states. Table III shows the order of weighting according to the Appendix, where the range ($x_1$, $x_2$ and $x_3$) has uncertainties on the order of 50 ft and the azimuth and elevation measurement ($x_5$ and $x_6$) uncertainties are five to seven magnitudes smaller at 2.E-3 rad to 2.E-5 rad.

Table IV has the best fit for the states $x_1$, $x_2$, and $x_3$ but the algorithm never converged. This can be explained by the extremely small weights for $x_5$ and $x_6$, thereby causing the algorithm to ignore these states when computing the performance index. For this reason, the parameter histories, which are very dependent upon the $x_5$ and $x_6$ states (see the state equations), did not converge to the proper values. The same reasoning applied to the Table V weights, for which the run did not converge. Therefore, although the weighting matrix for Table III had a less accurate fit to the experimental trajectory states $x_1$, $x_2$, and $x_3$, it is the matrix that most closely represents the true error model. The errors for the states in Table III are representative of the magnitude of the errors that can be achieved by this

41

algorithm while providing converged (good) parameter
histories.

## Run 3

The third run used data from the BET as the experimental values. As was previously mentioned, the BET
provides state history data which was used in this run.
Since the BET also provides the $C_L$ and $C_D$ histories for
this trajectory data, the converged algorithm should yield
similar parameter histories. This allows the algorithm to
"prove" itself against the BET's parameter estimation
procedure.

This run used 500 CP seconds to converge to $A = 1.E-7$,
$B = 6.E-5$, and $\alpha = 1$. The state time histories are
listed in Table VI. The initial and converged parameter
histories are portrayed in Figures 12, 13, and 14. Notice
that the bank angle fit was very good, as the accuracy of
the $x_5$ state history fit implies, although the initial and
converged parameter histories are significantly different
in magnitude. This shows the ability of the algorithm to
converge given a poor initial $\beta$ .

Because the lift to drag ratio (L/D) can be calculated
without the need for a reference area, s, and a weight, w,
the L/D for the converged $\beta$ was compared to the L/D values
given by NASA's BET, so that the comparison is only dependent
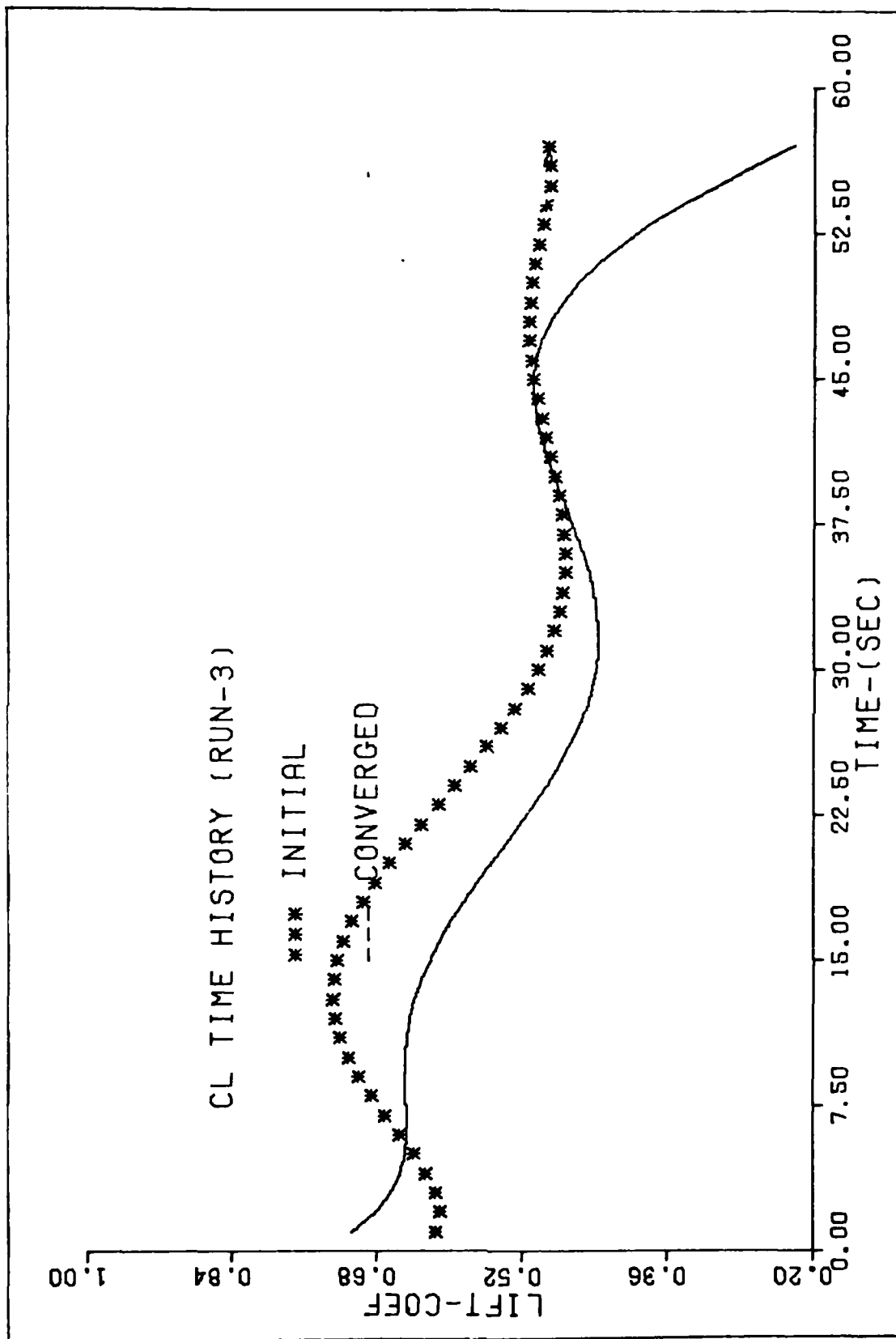
Fig..12. Initial and Converged $C_L$ (Run 3)

43
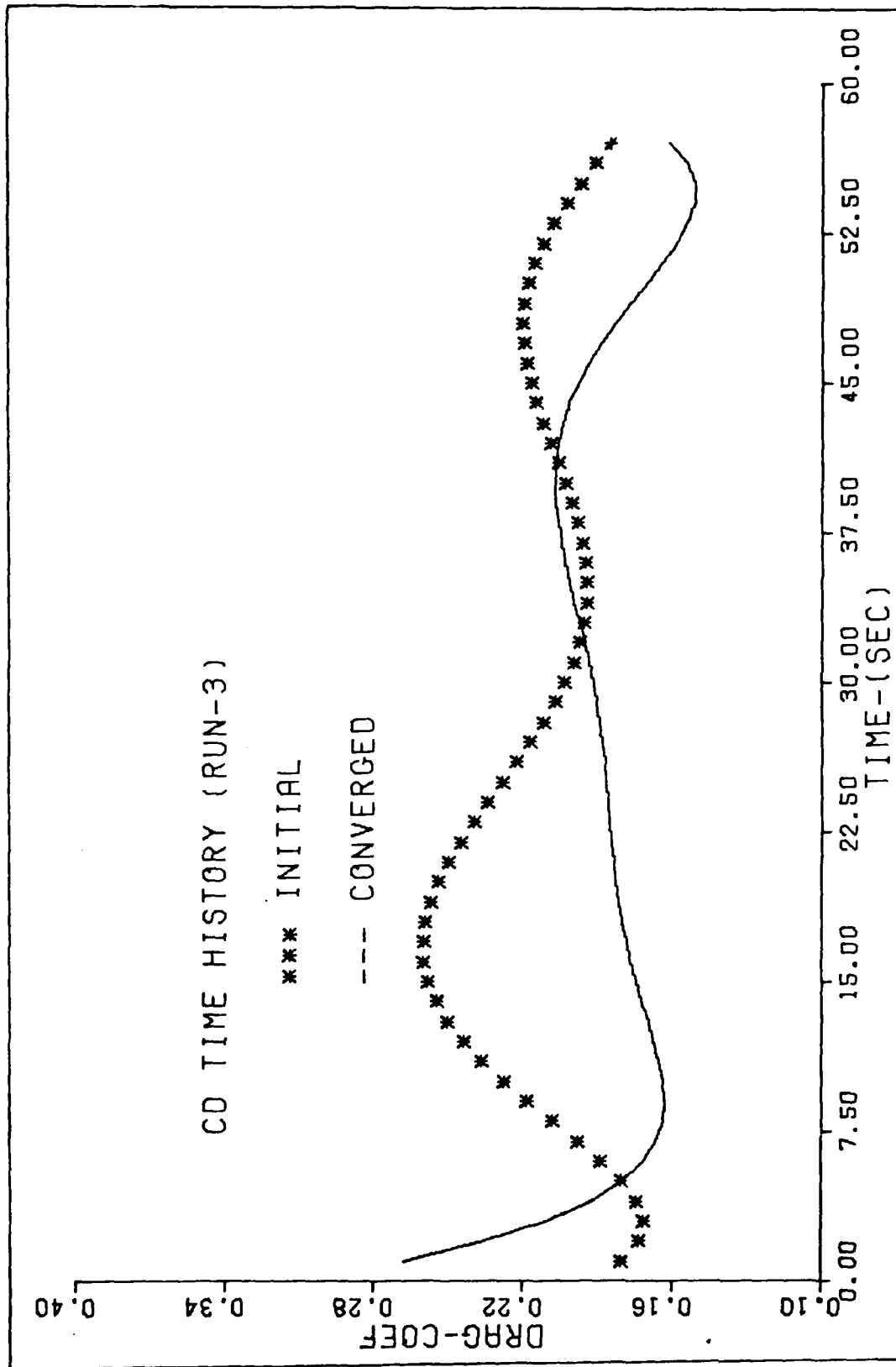
Fig. 13. Initial and Converged $C_D$ (Run 3)

44
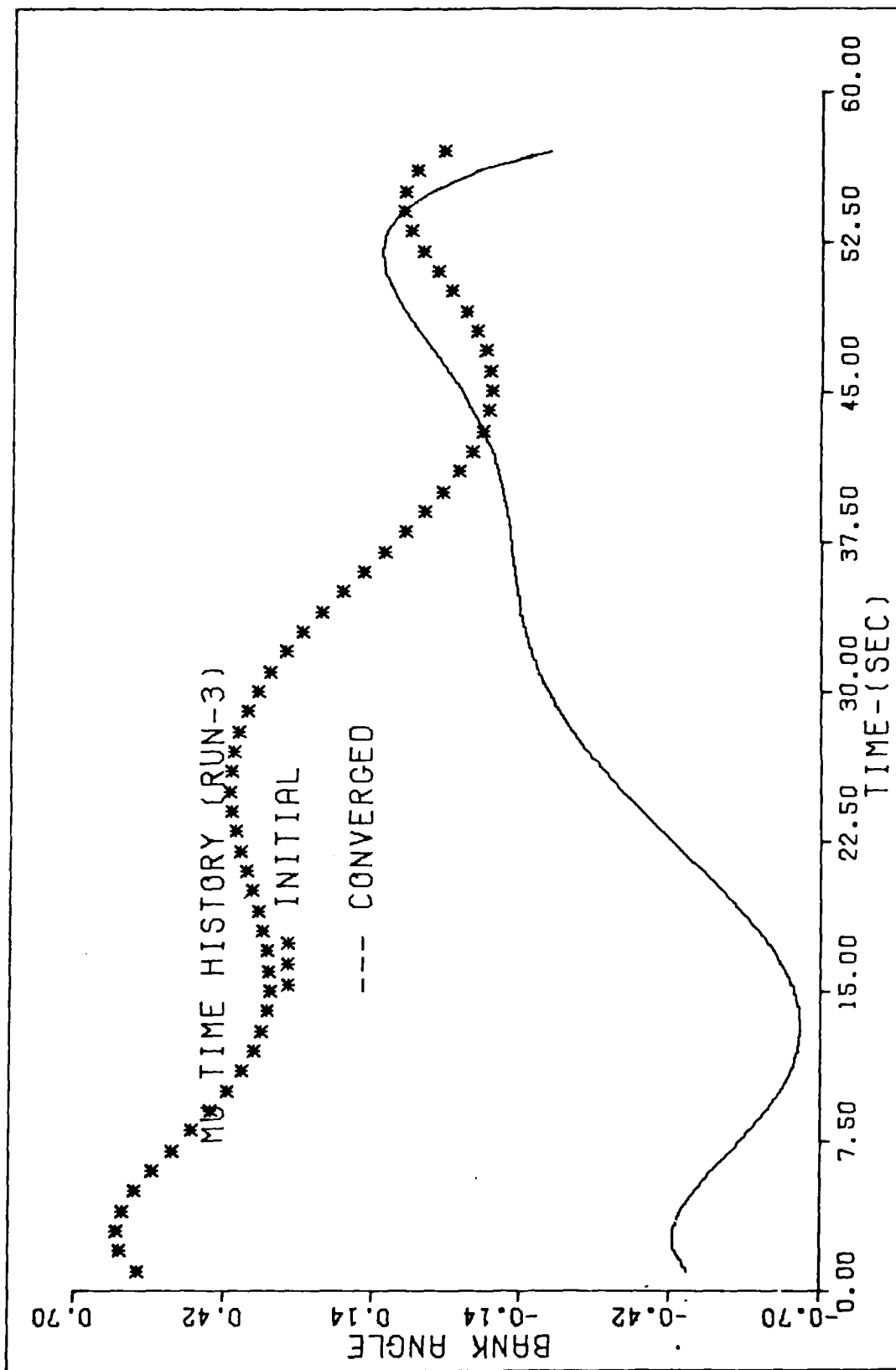
Fig. 14. Initial and Converged $\gamma$ (Run 3)

45

upon the two methods of parameter estimation. Figures 15
and 16 present in graphic form the comparisons of the
initial to the converged and the converged to the BET L/D
ratios, respectively. Figure 16 shows good correspondence
between the two methods of identifying the L/D ratio. The
BET L/D history is not restricted to be a smooth polynomial.
The beginning and end of the converged polynomial L/D
history does not correspond as well to the BET values.
This can be attributed to the assumption that $x_o$ was perfectly
known and to the use of polynomials of lower order than
may be necessary for the interval length (Figure 12, for
instance).
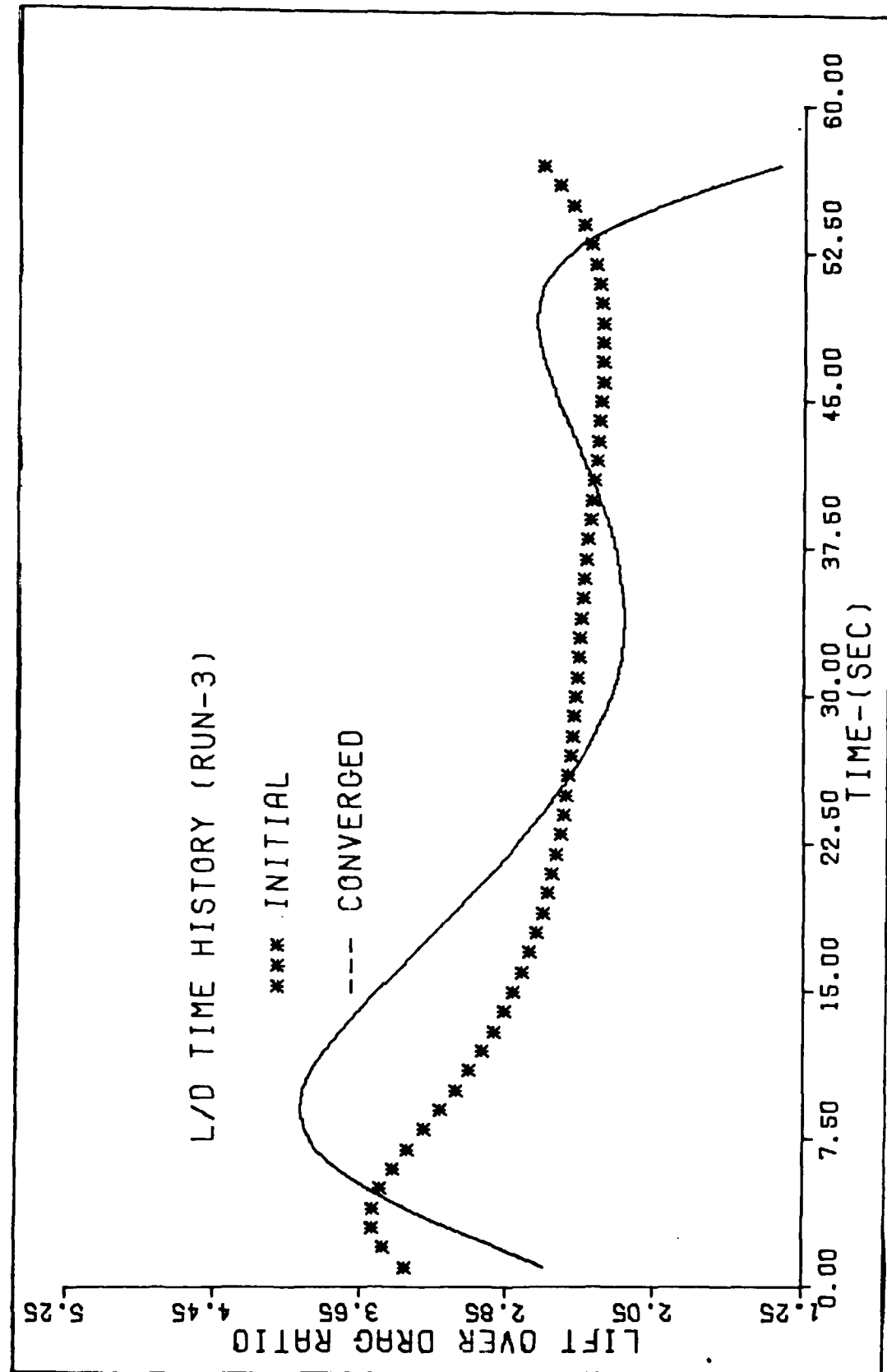
Fig. 15. Initial and Converged L/D (Run 3)
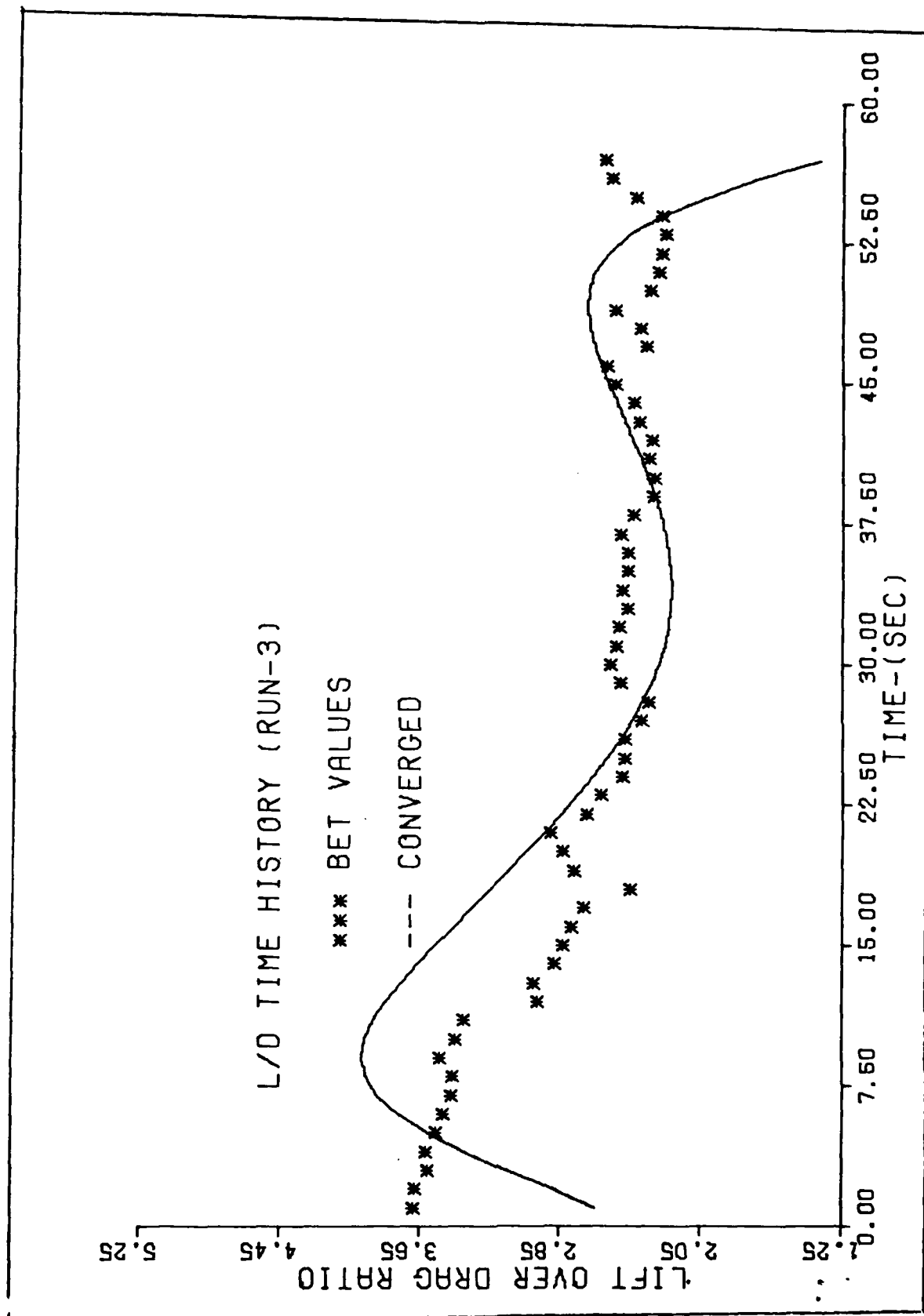
Fig. 16.   BET and Converged L/D (Run 3)

48

# V  Conclusion

Summary

This report presented a nonlinear parameter identification algorithm that was used to find $C_L$, $C_D$, and $\mu$ time histories, derived from radar trajectory data, for the Space Shuttle reentry.  The algorithm, a Square-Root Variable-Metric optimization technique, (Ref 4,9) provided a fast and inexpensive method for obtaining good results for the parameter histories, by minimizing the weighted least squares performance index, J, of the experimental versus calculated state histories.

There were several programming considerations discussed in Chapter III.  The procedure used to execute the one dimensional search was detailed, showing a need to manipulate the tolerances for convergence and to vary the step size when needed.  Finding the best numerical differentiation constant, $\in$ , was done by varying $\in$ until the most accurate estimate of the derivative was obtained.  This reduced errors due to computer round-off and central difference formula truncation.  Nondimensional polynomial coefficients were also used to reduce these errors.  Finally, by inverting the magnitude of the uncertainties given in the Appendix, the diagonal elements of the W matrix were chosen.

The results were presented and analyzed in Chapter IV.

Run 1 and Run 2 tested the mechanics of the algorithm dependent upon the choice of interval length, polynomial order, and weighting matrix. It was shown that the initial parameter histories were close enough to the converged values to give fairly rapid convergence. Run 3 used the BET parameters as a comparison to the converged solution using the BET state histories as the radar trajectory data. This showed good correspondence between the two estimation methods for a L/D ratio time history, hence, giving confidence in the algorithm's effectiveness (Fig. 16). It was noted that, because of the characteristics of polynomial approximation and the assumption that $x_0$ was fully known, the converged parameter histories may be inaccurate at the ends of the time intervals. All three runs converged well to the given experimental state histories (Tables I, II, and III), but not all of the parameter history characteristics were portrayed if the order of the polynomial fit did not match correctly with the interval length.

Computer time was short, about 500 CP seconds (hence, inexpensive) and was made shorter by choosing smaller order polynomials.

## Recommendations

This algorithm provides a relatively simple method for identifying parameter histories. The results for the nonlinear

state model, deterministic, Square-Root Variable-Metric
optimization routine corresponded well with the BET results
without the problems of matrix inversion. The computer
load is very manageable with 500 CP seconds as an average
time for fitting about a minute long interval with a sixth
order polynomial using the CDC Cyber 74.

Because the radar data is readily available for most
of the Space Shuttle reentry trajectory, this algorithm
could be useful for quickly yielding good parameter history
results. These results would allow evaluation of maneuvers
or unplanned motion without the long wait for NASA's BET.
This could perhaps be useful for speeding up the turn
around time between launches should any problems which
might arise during reentry need evaluation before the
next launch.

Redundant results are important when testing the
performance of a system. Using this parameter identifica-
tion process would give a second, redundant, means for
evaluating the accuracy of the BET data. Although NASA's
BET gives a full six DOF evaluation of the Space Shuttle's
reentry, such a comparison would inspire more confidence in
the BET results.

The method used here to identify parameters can also
be used where any parameters need to be found, as long as
an appropriate state model is given. The polynomial fits,

one-dimensional search development, and weighting matrix choice are all appropriate considerations whether using this or a similar optimization technique. Therefore, the results presented give insight to what can be achieved in the field of nonstochastic parameter identification.

Further work with this algorithm could explore the use of a full measurement covariance matrix inversion as the weighting matrix. This would more accurately describe the real world radar errors and thereby improve the accuracy of the algorithm. Also, the state model could be expanded to more accurately describe the Space Shuttle three DOF motion. Spherical Earth, wind, and noise modelling would all increase the accuracy of the model, but at some degree of expense to the speed of convergence, as the computational load increases due to a more complex dynamical system model. The trade-off of accuracy versus speed of convergence can be studied using the results of these further studies and the results presented in this report.

# Bibliography

1. "AFFTC Evaluation of the Space Shuttle Orbiter and Carrier Aircraft - NASA Approach and Landing Test," NASA, May 1978, AF Flight Test Center, Edwards AFB, California.

2. Bond, A.C., Jr. and J. Knoedler. "OFT Ascent/Descent Ancillary Data Requirements Document," Mission Planning and Analysis Division, NASA. Houston, Texas, February 1980.

3. Fox, R.L. Optimization Methods for Engineering Design. Addison-Wesley Publishing Co. Reading, Mass. 1971.

4. Gupta, N.K. and W.E. Hall, Jr. "System Identification Technology for Estimating Re-entry Vehicle Aerodynamic Coefficients," J. Guidance and Control: Volume 2, No. 2. 139-146 (March-April 1979).

5. Hull, D.G. and W.E. Williamson, Jr. "A Nonlinear Method for Parameter Identification Applied to a Trajectory Estimation Problem," AIAA Atmospheric Flight Mechanics Meeting, August 1977.

6. McDowell, J.L., B.E. Shutz and B.D. Tapley. "An Analysis of Reentry Vehicle Trajectory Reconstruction and Parameter Identification," Paper No. 1685, AIAA Flight Mechanics Conference, Boulder Co., August 1979.

7. Mendel, J.M. "Postflight Data Analysis by Means of Adaptive, Iterated, Extended Kalman Filtering," IEEE Transactions on Automatic Control, Volume AC-19. No. 5. (October 1974).

8. NASA. "Best Estimated Trajectory No. 2," Magnetic Tape received through Jim Hayes, Flight Dynamics Lab, Wright Patterson, AFB, Ohio.

9. Tejeda, J. "Multisensor Space Position Report, Ops. No. 104-80, Mission Date 14 April 1981," Kentron International Inc., prepared for Data Production Branch, Computer Sciences Division, 6520 Test Group, Air Force Flight Test Center, Edwards, AFB, California, April 1981.

10. Williamson, W.E. "Square-Root Variable-Metric Method for Function Minimization," AIAA Journal, Volume 13, No. 1. 107-109 (1975).

## Appendix

The following four tables are from Reference 8.
The first two tables, C-1 and C-2, show the weights and
apriori bias information for the Multisensor Report data.
Tables D-1 and D2 show the radar measurement mean and
uncertainties.  The diagonal elements for the weighting
matrix were arrived at by combining the bias and uncertainty
magnitudes and inverting them.  The first three diagonal
elements, representing states $x_1$, $x_2$, and $x_3$, are weighted
from the range magnitude and the last two diagonal elements,
representing $x_5$ and $x_6$, are weighted from the azimuth and
elevation magnitudes.  The fourth diagonal element, repre-
senting the weighting of the $x_4$ (velocity) state, was
given a value of magnitude between the range and azimuth
magnitudes since Doppler residual statistics were not
provided.

| SENSOR WEIGHTS AND APRIORI BIAS INFORMATION FOR RUN NO. 1 | | | | | | | | |
|---|---|---|---|---|---|---|---|---|
| **SENSOR** | **WEIGHTS** | | | **BIASES** | | | **BIAS UNCERTAINTIES** | | |
| | RANGE (FEET) | AZIMUTH (DEG) | ELEV. (DEG) | RANGE (FEET) | AZIMUTH (DEG) | ELEV. (DEG) | RANGE (FEET) | AZIMUTH (DEG) | ELEV. (DEG) |
| FPS16/38 | 30.00 | .008 | .008 | 19.52 | .00474 | .00837 | 63.09 | .03261 | .03266 |
| NASA FPS16 | 30.00 | .008 | .008 | 10.41 | .00065 | .01140 | 58.62 | .03307 | .02606 |
| TPQ18 SA 48 | 30.00 | .008 | .008 | -38.25 | .01682 | .01991 | 65.66 | .02749 | .02993 |
| C1 | 0.00 | .003 | .003 | 0.00 | -.00143 | -.00163 | 0.00 | .00524 | .00344 |
| C4 | 0.00 | .003 | .003 | 0.00 | .00318 | -.00159 | 0.00 | .00407 | .00383 |
| C5 | 0.00 | .003 | .003 | 0.00 | -.00139 | -.00197 | 0.00 | .00496 | .00287 |
| C6 | 0.00 | .003 | .003 | 0.00 | .00574 | -.00191 | 0.00 | .01010 | .00435 |
| C7 | 0.00 | .003 | .003 | 0.00 | -.00379 | .00296 | 0.00 | .00627 | .00509 |

TABLE C-1

| BIAS ESTIMATION RESULTS AND UNCERTAINTIES FOR RUN NO. 1 | | | | | | |
|---|---|---|---|---|---|---|
| **SENSOR** | **BIASES** | | | **BIAS UNCERTAINTIES** | | |
| | RANGE (FEET) | AZIMUTH (DEG) | ELEVATION (DEG) | RANGE (FEET) | AZIMUTH (DEG) | ELEVATION (DEG) |
| FPS16/38 | 27.87364 | .00109 | .02611 | 1.38904 | .00035 | .00039 |
| NASA FPS16 | 17.88180 | -.00161 | .02940 | 1.29678 | .00033 | .00039 |
| TPQ18 SA 48 | -27.56410 | .01939 | .04245 | 1.76858 | .00038 | .00044 |
| C1 | 0.00000 | -.00712 | .00680 | .00000 | .00026 | .00033 |
| C4 | 0.00000 | .00281 | .00476 | .00000 | .00019 | .00026 |
| C5 | 0.00000 | -.00280 | .00504 | .00000 | .00021 | .00027 |
| C6 | 0.00000 | .00632 | .00498 | .00000 | .00020 | .00025 |
| C7 | 0.00000 | -.01127 | .01350 | .00000 | .00029 | .00036 |

TABLE C-2

55

| SENSOR | RESIDUAL STATISTICS FOR RUN NO. 1 | | | | | |
|---|---|---|---|---|---|---|
| | MEAN | | | UNCERTAINTIES | | |
| | RANGE (FEET) | AZIMUTH (DEG) | ELEVATION (DEG) | RANGE (FEET) | AZIMUTH (DEG) | ELEVATION (DEG) |
| FPS16/38 | .00273 | -.00000 | .00000 | 61.20924 | .03209 | .02937 |
| NASA FPS16 | .00252 | -.00000 | .00000 | 59.67920 | .03065 | .02285 |
| TPQ18 SA 48 | .00404 | .00000 | .00000 | 64.70393 | .02703 | .02392 |
| C1 | - | -.00000 | .00002 | - | .00521 | .00315 |
| C4 | - | -.00000 | .00001 | - | .00438 | .00392 |
| C5 | - | -.00000 | .00002 | - | .00476 | .00285 |
| C6 | - | .00000 | .00001 | - | .01114 | .00439 |
| C7 | - | -.00000 | .00001 | - | .00639 | .00427 |

TABLE D-1

| POSITIONAL UNCERTAINTY STATISTICS FOR RUN NO. 1 | | |
|---|---|---|
| COORDINATE | MEAN (FEET) | UNCERTAINTIES (FEET) |
| R SPHERICAL ERROR | 43.76213 | 60.96327 |
| X TOTAL | 14.33824 | 15.27715 |
| Y TOTAL | 25.19341 | 38.38616 |
| Z TOTAL | 31.88084 | 45.47689 |
| X RANDOM | 14.31515 | 15.25862 |
| Y RANDOM | 25.15378 | 38.33737 |
| Z RANDOM | 31.80159 | 45.39780 |
| X SYSTEMATIC | .80540 | .76054 |
| Y SYSTEMATIC | 1.39732 | 1.94573 |
| Z SYSTEMATIC | 2.17653 | 2.73815 |

TABLE D-2

## VITA

Harry Francis Johnson was born December 25, 1957, in Atlantic City, New Jersey. He graduated from high school in Ramsey, New Jersey, in 1976 and attended the University of Colorado until December, 1978. He transferred to the University of Illinois, from which he received the degree of Bachelor of Science in Aeronautical and Astronautical Engineering in May, 1980. He entered the Air Force and the School of Engineering, Air Force Institute of Technology, in June, 1980. He is an Engineer-in-Training in the State of Ohio.

Permanent address: 1027 Shambliss Ct.
Buffalo Grove, IL 60090

| REPORT DOCUMENTATION PAGE | | READ INSTRUCTIONS BEFORE COMPLETING FORM |
|---|---|---|
| 1. REPORT NUMBER AFIT/GA/AA/81D-7 | 2. GOVT ACCESSION NO. AD-A111 121 | 3. RECIPIENT'S CATALOG NUMBER |
| 4. TITLE (and Subtitle) NONLINEAR PARAMETER IDENTIFICATION LIFT COEFFICIENT, DRAG COEFFICIENT, AND BANK ANGLE HISTORIES FOR THE SPACE SHUTTLE TEST FLIGHT I | | 5. TYPE OF REPORT & PERIOD COVERED |
| | | 6. PERFORMING ORG. REPORT NUMBER |
| 7. AUTHOR(s) Harry F. Johnson, 2d Lt, USAF | | 8. CONTRACT OR GRANT NUMBER(s) |
| 9. PERFORMING ORGANIZATION NAME AND ADDRESS Air Force Institute of Technology (AFIT/EN) Wright-Patterson AFB, OH 45433 | | 10. PROGRAM ELEMENT, PROJECT, TASK AREA & WORK UNIT NUMBERS |
| 11. CONTROLLING OFFICE NAME AND ADDRESS Department of Aeronautics and Astronautics (AFIT/ENY) Wright-Patterson AFB, OH 45433 | | 12. REPORT DATE December 1981 |
| | | 13. NUMBER OF PAGES 66 |
| 14. MONITORING AGENCY NAME & ADDRESS(if different from Controlling Office) | | 15. SECURITY CLASS. (of this report) Unclassified |
| | | 15a. DECLASSIFICATION DOWNGRADING SCHEDULE |

16. DISTRIBUTION STATEMENT (of this Report)

Approved for public release; distribution unlimited

17. DISTRIBUTION STATEMENT (of the abstract entered in Block 20, if different from Report)

APPROVED FOR

2

18. SUPPLEMENTARY NOTES

20. ABSTRACT (Continue on reverse side if necessary and identify by block number)

A nonlinear, Square-Root Variable-Metric optimization
technique is used to extract time histories for the lift
coefficient, drag coefficient, and bank angle control variables
from radar data of the Space Shuttle Test Flight I. This
optimization technique solves for these control variable his-
tories by minimizing a weighted least squares performance
index of the calculated versus experimental state equation

19. KEY WORDS (Continue on reverse side if necessary and identify by block number)

Nonlinear Parameter Identification
Space Shuttle

DD FORM 1473 EDITION OF 1 NOV 65 IS OBSOLETE
1 JAN 73

time histories. The state model is a three degree of freedom representation of aircraft motion.

Three intervals of data are evaluated. In each interval, polynomial functions represent the control variables, and the performance index is dependent only on the values of the polynomial coefficients. The larger of the first two intervals contained the shorter interval so that the effect of changing polynomial order and interval length could be explored. The third interval compared the calculated parameter histories with NASA's BET parameter histories with good correspondence. For all three intervals the calculated state histories closely matched the experimental state histories.

These results show that given an appropriate state model, this optimization technique is useful for quickly obtaining good and inexpensive estimates of certain desired parameters.

# END

## DATE
## FILMED

3-82

## DTIC